

ORIGINAL ARTICLE

Advancing Domestic Freezers With Phase Change Materials: Experimental Study Towards Commercialization

Daniel Marques¹  | Vitor Silva² | Nelson Martins¹  | Fernando Neto¹ 

¹Centre for Mechanical Technology and Automation (TEMA), Department of Mechanical Engineering, University of Aveiro, Campus Universitário de Santiago, Aveiro, Portugal | ²Tensai Indústria, S.A., Avenida Cidade de Estarreja, n° 1 Eco-Parque Empresarial de Estarreja, Estarreja, Portugal

Correspondence: Daniel Marques (danielmarques11@ua.pt)

Received: 3 October 2024 | **Revised:** 10 February 2025 | **Accepted:** 1 March 2025

Funding: This work was supported by the Fundação para a Ciência e a Tecnologia (FCT), the Portuguese National Foundation for Science and Technology (grant number 2021.06083.BD) and by the projects UIDB/00481/2020 and UIDP/00481/2020—Fundação para a Ciência e a Tecnologia, DOI 10.54499/UIDB/00481/2020 (<https://doi.org/10.54499/UIDB/00481/2020>) and DOI 10.54499/UIDP/00481/2020 (<https://doi.org/10.54499/UIDP/00481/2020>), and CENTRO-01 0145-FEDER-022083 under the program “Centro Portugal Regional” (Centro2020), and the PORTUGAL 2020 partnership agreement, through the European Regional Development Fund.

Keywords: chest freezers | cold energy storage | domestic refrigeration systems | experimental research | industrialization | phase change materials | system design

ABSTRACT

The urgency for more efficient and sustainable domestic refrigeration systems (DRSs) is intensifying due to climate change events like more frequent heat waves. Such challenges impose reducing greenhouse gas emissions, increasing renewable energy storage rates, meeting the perishable food needs for cooling, and mitigating food wastage through power outages. While previous investigations contributed to these goals by studying the potential benefits of adding phase change materials (PCMs) to DRSs, our study extends their application to chest freezers: a type of system still underexplored. Additionally, it seeks to enhance industrialization and design decision-making towards tailoring different solutions to distinct markets. Namely, by adopting test procedures closely adhering to the European Standard EN 62552:2013 for experimentally testing four prototypes. The analysis of the novel systems' performance focuses on two metrics internationally recognized but scientifically overlooked by previous peer research: the temperature rise time and the daily energy consumption. A novel approach for filling the top-mounted door with PCMs and an industrialization technique for simultaneous wrapping PCM bags and evaporator tubes around the freezer compartment are introduced to incorporate PCMs, with melting temperatures (T_m) of -21°C and -12°C . Our findings reveal the potential to extend blackout autonomy by 7%–40% and to reduce daily energy consumption by 13%. Furthermore, the results demonstrate that higher T_m values enhance the commercial attractiveness of DRSs in regions with unstable electricity grids where significant autonomy gains are appreciated, while lower T_m values suit sophisticated markets where extended energy storage capacity and compressor lifetime can be prioritized.

1 | Introduction

Essential human needs, such as food preservation and safety, heavily rely on cold generation, as 45% of the universally produced

food requires low-temperature storage and distribution to avoid waste and combat hunger [1]. In 2019, 2 billion domestic refrigerators/freezers were estimated to be operating worldwide, accounting for 4% of the global electricity consumption [2, 3].

Abbreviations: AC, alternate current; COP, coefficient of performance; DC, direct current; EN, European norm; PCMs, phase change materials; VCR, vapor compression refrigeration.

Furthermore, climate change impacts, including more frequent heat waves and recurring power outages in areas with unstable electricity grids, affect food security in developing nations, where frozen food and electrical devices are at risk of spoilage [4, 5]. In countries like India, less than 35% of perishable food is adequately cooled [3]. Consequently, the demand for domestic refrigeration systems (DRSs) is rapidly growing, with annual production now exceeding 80 million units, and the compound annual growth rate for the cold chain market is projected to reach 8.30% by 2030 [6–9].

Given that energy efficiency can contribute to 44% of the reduction in CO₂ emissions required by the Paris Agreement, advancing towards efficient and sustainable refrigeration is critical [10]. Phase change materials (PCMs) stand out for this purpose through their ability to store 5–14 times more heat per unit of volume as latent heat than sensible heat methods, making them attractive for improving DRSs [11].

Accordingly, several experimental studies have tested PCM integration in cooling units, namely, at the evaporator and within compartments for low-temperature latent cold storage, to validate the concept and assess the potential benefits of its use. These are summarized as follows.

1.1 | Temperature Stability and Autonomy Extension With PCMs

- Kiran-Yildirim [12] explored using PCMs with melting points (T_m) of 0°C and −1.2°C in the single fresh-food cabinet of a laboratory-scale system. During 6-h blackouts, the time for internal air to rise from 0°C to 20°C increased by up to 380% with PCM integration.
- Riffat et al. [13] tested a domestic refrigerator with PCMs ($T_m = 4^\circ\text{C}$) designed for rural areas with weak or missing power grids, observing that during 5-h power outages at an ambient temperature of 33.8°C, the air inside its single fresh-food compartment also gently rose from 7°C to 11°C, suggesting enhanced food safety.
- Liu et al. [14] added water with nucleating agents ($T_m = 0.41^\circ\text{C}$) to the refrigerated section and a NaCl aqueous solution ($T_m = -18.98^\circ\text{C}$) to the freezer of a domestic unit. With PCMs, the refrigerated section stabilized below 8°C for six out of the 8 h of the predefined length of power cuts, while the freezer section held test packages under −18°C for an additional hour compared with the setup without PCMs.
- Antony Forster Raj and Joseph Sekhar [15] observed smoother temperature fluctuations by placing PCMs between the evaporator coil and polyurethane insulation of a small-scale, single-compartment, vapor compression refrigeration (VCR) system. With PCMs melting at $T_m = 0^\circ\text{C}$ or −16°C, preparing their system to operate as a refrigerator or freezer, the average temperature rise rate reduced from 2°C/h to 0.4°C/h, with a test procedure started after switching OFF the compressor at a cabinet temperature of −16°C.
- Sonnenrein et al. [16] integrated PCMs ($T_m = 9^\circ\text{C}$) into the fresh-food compartments of refrigerating units, achieving autonomy extension in the time for the cabinet to rise from 8°C to 11°C of up to 145%.
- Husainy et al. [17] used a nanoenhanced eutectic PCM (KCl + Na₂SO₄ + graphene) in a refrigeration test rig, which helped maintain the cabinet temperature stable between 7°C and 9°C for up to 15 h, while without using PCMs, the temperature rose to 22°C within the same time period.
- Radebe et al. [18] studied three PCMs with T_m of −10°C, −19°C, and −21°C within the freezer compartment of a refrigerator, finding that they maintained the fresh-food cabinet temperature below 4°C during 2.5-h power outages in South Africa.
- Oró et al. [19, 20] evaluated a vertical freezer where stainless-steel cases encapsulating PCMs with melting points of −18°C or −21°C were placed in the trays above the evaporator tubes. During 3-h power outages, the PCM-enhanced unit kept the test packages 2°C colder than the ordinary freezer, while for longer blackouts of 6, 12, and 24 h, the frozen food temperatures remained 4°C–6°C lower.
- Mane and Patil [21] observed the temperature rise time of a domestic refrigerator without PCMs and with one of three eutectic PCMs. The time after the power cut-off until the cabin air temperature reached 16.6°C, called the backup time, was measured and increased by 14%–182% with the inclusion of PCMs in distinct configurations, namely, varying their mass.

1.2 | Energy Consumption Reduction and Coefficient of Performance (COP) Improvement

- Yusufoglu et al. [22] separately examined the impact of PCMs with T_m of 0°C, −2.5°C, −3.6°C, or −4.4°C placed at the evaporator of single-compartment refrigerators. Their findings revealed energy savings of 9.4%, a COP improvement of 17.4%, and a 5% decrease in the running time ($\text{ON}_{\text{time}}/\text{Cycle}_{\text{time}}$), suggesting the potential for a longer compressor lifespan through less cycling.
- Khan and Afroz [23, 24] observed that water or eutectic PCMs (with $T_m = -5^\circ\text{C}$) in a refrigerator similar to the tested by Yusufoglu et al. boosted the COP by 20%–27% and cut compressor cycling by 3–5 times.
- Cofré-Toledo et al. [25] recorded a 9% reduction in compressor running time in a two-door, domestic unit with an E-10 commercial mixture or 19.5 wt% NH₄Cl aqueous solution at the evaporator.
- Antony Forster Raj and Joseph Sekhar [15] experiments under an ambient temperature of 32°C to system operation without load yielded COP increases of up to 17.4%, along with daily energy demand savings of up to 17.31%.
- Sonnenrein et al. [16] reported daily energy consumption (kW.h/24 h) reductions of 1.6% and cooling time reductions of up to 33% in the cooling capacity test, which evaluates

the time needed to cool the test packages from 25°C to 10°C. This was due to a temperature homogenization within the compartment while the selected PCMs were freezing at 9°C.

- Padhye and Agrawal [26] conducted experiments integrating a salt solution (10% NaCl + 90% H₂O by wt) or a eutectic solution (25% C₂H₆O₂ + 75% H₂O by vol.) into the freezer of a single-door refrigerator freezer. Adding PCMs reduced compressor ON/OFF cycles by 50%–80%.
- Rahimi et al. [27] experimentally tested the inclusion of PCM slabs with different metallic materials in a single-door refrigerator, focusing on thermal conductivity enhancement using aluminum, steel, or copper fins. Overall energy consumption was reduced by 13.7% when using copper fins.
- Abdolmaleki et al. [28] achieved an 8.37% decrease in energy demand by using polyethylene–glycol eutectic solutions in a vertical freezer, which also helped stabilize internal temperatures.
- Joseph Sekhar et al. [29] used an experimental setup of a 210-L refrigerator and a 250-L chest freezer, both containing PCMs with T_m of 3°C, −15.4°C, or −18°C, connected to an array of PV panels. PCM use revealed it could reduce energy consumption by 8%–15% during night hours.
- Jasim et al. [30] experimented using water as PCM at the back of the evaporator or within the compartment of a household refrigerator. Over a 24-h experiment, they observed a 21.97% increase in the system COP and a 14.4% reduction in energy consumption, mainly due to an extended compressor OFF time of up to 73 min.
- Pharande and Desai [31] covered the evaporator of a single-door household refrigerator with a copper or steel casing filled with ethylene glycol–water mixture as PCM, achieving COP improvements of 15%–18% and energy consumption cuts of 14.50%–17.47%.
- Pirvaram et al. [32] tested different combinations of two eutectic PCMs melting at −18°C and −20°C implemented in a cascade-like arrangement on six trays of a single-door, three-star vertical freezer. This setup reduced the freezer's energy consumption by 12.31%.

The prior experimental studies cited demonstrate promising results and potential benefits from integrating PCMs into DRSs, including reduced energy consumption through COP improvement and running time decrease, the extended compressor's lifespan, and enhanced temperature stabilization. The latter excels during electricity blackouts, extending the period for food to remain safely frozen or refrigerated. Such findings suggest that future domestic VCR systems with PCMs could become more efficient and sustainable while offering a means for latent thermal energy storage that could also accommodate renewable energy.

While these are valuable references, only a few studies have adopted established international testing standards in which technical datasheet specifications of DRSs required for commercialization are defined. Yusufoglu et al. [22] partially adopted the testing methods for household refrigerating appliances specified by the International Standard IEC 62552:2015

[33–35] in their energy consumption analysis. Sonnenrein et al. [16] also referenced the IEC 62552:2015 standard despite adopting unspecified, empirical criteria for claiming the temperature rise time extensions. Others employed local standards and focused solely on energy consumption analysis, such as Cofré-Toledo et al. [25], partially adopting the Colombian Technical Standard NTC5891, and Rahimi et al. [27], Abdolmaleki et al. [28], and Pirvaram et al. [32] opting for the Iranian ISIRI 13700 testing guidelines.

By not fully adhering to standardized testing, much of the current experimental research lacks critical insights into relevant metrics for market scaling and commercializing PCM-enhanced systems. Namely, the daily energy consumption—key to determining the systems' energy-efficiency label—and the systems' autonomy—defined as the time that food remains safely frozen within −18°C to −9°C inside a freezer under power outages—are two key metrics that have been overlooked in scientific research.

Moreover, these regulations are universally recognized by manufacturers and governing bodies for evaluating the performance of household cooling appliances, making them a benchmark for comparing PCM-enhanced DRSs. These enable reputable comparisons of the effects of different PCM configurations (e.g., varying mass and melting point) from the perspective of the technical datasheet specifications, an analysis that none of the cited authors executed and which is an objective met in this paper.

This study aims to address these gaps by conducting a rigorous evaluation of the impacts of PCM integration in chest freezers, a DRS type less examined for this purpose in the cited references. For that, we developed and tested four chest freezer prototypes incorporating commercially available PCMs at the evaporator and system door, mostly varying mass and melting points. Two PCMs, with $T_m = -21^\circ\text{C}$ and -12°C , were selected given their compatibility with the systems' operational temperature range.

We opted for closely adhering to the test procedures established at the European standard EN 62552:2013 [36–38], which had been used at the certification date to commercialize the original model without PCMs. This standard includes the guidelines for quantifying the daily energy consumption and temperature rise time, the two metrics for which the prototypes are compared.

This methodological rigor allowed us to conduct a comparative analysis to evaluate the impacts of integrating PCMs in domestic refrigeration, focusing on advancing the concept closer to market commercialization readiness. Namely, we examine the commercial attractiveness of each prototype, discussing which designs might appeal to sophisticated economies or to developing countries based on the associated market priorities.

2 | Materials and Methods

This section describes the materials and procedures used in the present study. It begins with selecting the ordinary chest freezer

model and then discussing the chosen PCMs and the specific characteristics of the four prototypes developed for adding extra latent thermal energy storage capacity. The testing methodology, which adheres to the requirements from EN 62552:2013 for household refrigerating appliances, is then introduced. This includes a description of the thermophysical characteristics of the test packages, the associated load plan, and the data collection equipment.

2.1 | Ordinary Chest Freezer

The experiments were conducted using a horizontal chest freezer, model TCHEUSI180, which served as the ordinary refrigeration unit without PCMs. Table 1 summarizes the main characteristics of this commercially available freezer, as provided by the manufacturer, TENSAI Indústria [39, 40].

The TCHEUSI180 is a four-star freezer, which, according to EN 62552:2013 [36–38], holds a four-star compartment suitable for freezing foodstuffs from ambient temperature down to -18°C , and which is also suitable for storing frozen food under three-star storage conditions. This provides additional functionality compared with a three-star compartment, which is classified only as a frozen-food storage compartment and does not support freezing from ambient temperatures.

The system was modified by replacing the original fixed-speed compressor with a Secop BD80CN variable-speed compressor, which uses the refrigerant R290 in place of R600, as compared with the commercially available unit by TENSAI [41, 42]. The refrigerant and compressor replacement without modifying the rest of the VCR cycle allowed the freezer to reach lower evaporator temperatures, required to fully solidify PCMs with $T_m \leq -20^{\circ}\text{C}$ —enabling studying latent thermal energy storage solutions across a range of lower temperatures and which exhibit supercooling effects and thus require a colder heat sink.

Additionally, the variable-speed compressor can be directly connected to a photovoltaic panel, preparing the setup for future publications in which we will aim to test PCM-enhanced prototypes under distinct renewable energy supply scenarios. Figure 1 shows the adapted chest freezer, including a detailed view of the compressor enclosure housing the electronic control unit, which supports both alternate current and direct current power sources.

2.2 | Selecting PCMs

In any application, it is essential to align the system's operational requirements with the thermophysical properties of the heat storage materials for selecting PCMs. The phase change temperature must match the devices' operational temperature

TABLE 1 | Characteristics of the ordinary chest freezer [39, 40].

Property	Value
Height (mm)—interior/exterior	860/880
Width (mm)—interior/exterior	890/950
Depth (mm)—Interior/exterior	690/710
Polyurethane Insulation thickness (mm)—average	90
Polyurethane Insulation density (kg/m^3)—average	31.5
Net freezer volume (L)	165
Climatic class	T
Compartment classification	Four-star freezer compartment
Defrost system	No

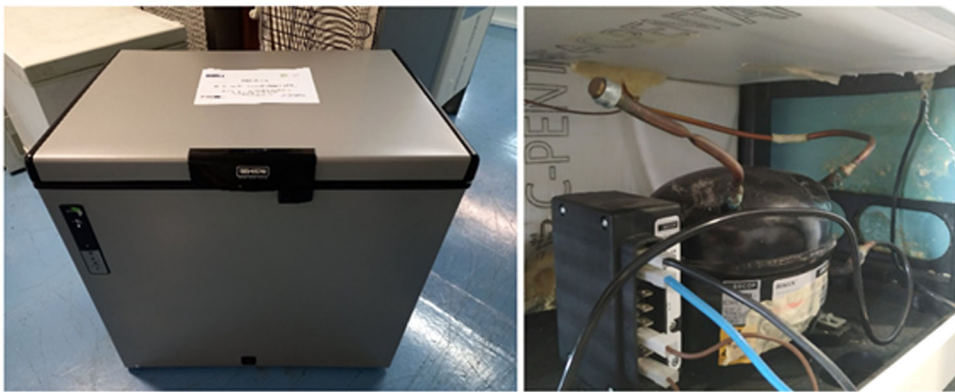


FIGURE 1 | (Left) Ordinary chest freezer model TCHEU180SI by TENSAI Indústria and (Right) application of the BD80CN variable-speed compressor with an electronic control unit for alternate current or direct current powering.

range, especially since temperature fluctuations inside refrigerated or frozen compartments must be restricted to $\pm 3^{\circ}\text{C}$ [43].

For domestic refrigeration units, if PCMs are installed at the evaporator or within compartments, their melting temperatures must fall between -30°C and $+8^{\circ}\text{C}$. This range reflects the minimum evaporator temperature, typically not lower than -40°C , and the storage temperatures of fresh-food compartments, which should not exceed 8°C [33–35]. Moreover, the minimum melting point for fresh-food compartments is constrained by the threshold that prevents sensible food items such as vegetables and fruit from freezing. So, water and eutectic PCMs have been predominant in previous research on cold storage PCMs applied in DRSS, while alternative aqueous solutions, including glycerol–ethanol or ethylene glycol, are promising for future studies [44–50].

Additional desirable PCM characteristics for this application include high melting enthalpy, low volume changes, long-term chemical stability, minimal supercooling, and low corrosiveness. These qualities help maximize energy storage capacity, extend systems' lifespan, and ensure energy efficiency [51–54]. In this study, we selected two commercially available PCMs from Cool SAS with melting points below the upper limit for frozen food safety during power outages, which is -9°C [36–38, 55, 56]. Namely, the eutectic gels COOL -21°C and COOL -12°C , designated as PCM_A and PCM_B, respectively, were chosen [57, 58].

Table 2 outlines their thermophysical properties as provided by the manufacturer.

While the manufacturer provided only three thermophysical properties of the selected PCMs for this study, other unknown properties were estimated using a similarity-weighted averaging approach. The method relies on selecting a set of reference materials that closely match the target PCM in the known properties (e.g., melting point, enthalpy of fusion, and density at liquid phase). To quantify similarity, the Euclidean distance was computed after normalizing the known values to ensure fair comparison across different property scales.

Then, materials with smaller distances were assigned higher weights, calculated as the inverse of the distance, and subsequently normalized to ensure the sum of all weights was equal to one. The missing properties of the target PCMs were then estimated as a weighted average of the corresponding properties from the reference materials. If a reference material lacked a value for a given property, it was excluded from the weighted averaging for that specific property, with the remaining weights re-normalized accordingly. This approach provided a systematic and quantitative method for property estimation based on data-driven similarity metrics.

Hence, using the thermophysical properties of four reference PCMs for each of the target PCMs (PCM_A and PCM_B), which are detailed in Tables 3 and 4, the values for the missing

TABLE 2 | Thermophysical properties of the selected PCMs.

PCM/property	PCM_A (COOL -21°C) [57]	PCM_B (COOL -12°C) [58]
<i>Manufacturer specifications</i>		
Melting point ($^{\circ}\text{C}$)	-21	-12
Enthalpy of fusion (kJ/kg)	266.60	269.27
Density at liquid phase (kg/m^3)	1151	1122
<i>Estimated properties</i>		
Density at solid phase (kg/m^3)	1145	1107
Thermal conductivity liquid ($\text{W/(m}\cdot\text{K)}$)	0.62	0.62
Specific heat liquid ($\text{kJ/(kg}\cdot\text{K)}$)	3.37	3.45
Specific heat solid ($\text{kJ/(kg}\cdot\text{K)}$)	1.87	2.30

Abbreviation: PCM, phase change material.

TABLE 3 | Reference PCMs and corresponding thermophysical properties to estimate PCM_A unknown properties.

Property/PCM	Pluss HS21N [59]	Rubitherm SP-21 [60]	PCM products E-21 [61]	Insolcorp DuraTemp-21 [62]
Melting point ($^{\circ}\text{C}$)	-21	-21	-21	-21
Enthalpy of fusion (kJ/kg)	1155	1200	1140	1100
Density at liquid phase (kg/m^3)	254	285	285	240
Density at solid phase (kg/m^3)	1078	1300	N/A	1150
Thermal conductivity liquid ($\text{W/(m}\cdot\text{K)}$)	0.7	0.6	0.51	0.6
Specific heat liquid ($\text{kJ/(kg}\cdot\text{K)}$)	3.4	N/A	3.13	3.7
Specific heat solid ($\text{kJ/(kg}\cdot\text{K)}$)	1.58	N/A	N/A	2.7

Abbreviations: N/A, not available; PCM, phase change material.

TABLE 4 | Reference PCMs and corresponding thermophysical properties to estimate PCM_B unknown properties.

Property/PCM	Pluss HS10N [63]	Rubitherm SP-11 [64]	PCM products E-11 [61]	Insolcorp DuraTemp-12 [62]
Melting point (°C)	−10	−11	−12	−12
Enthalpy of fusion (kJ/kg)	1125	1200	1090	1100
Density at liquid phase (kg/m ³)	290	290	310	302
Density at solid phase (kg/m ³)	1057	1100	N/A	1150
Thermal conductivity liquid (W/(m-K))	0.602	0.6	0.57	0.7
Specific heat liquid (kJ/(kg-K))	3.4	N/A	3.55	3.4
Specific heat solid (kJ/(kg-K))	1.9	N/A	N/A	2.6

Abbreviations: N/A, not available; PCM, phase change material.

TABLE 5 | Type, mass, and location of the PCMs employed in each chest freezer prototype.

Prototype	Type of PCM	Mass of PCM (kg)	Additional latent thermal energy storage capacity (kJ)	PCMs' location
CF_1	PCM_A	6.8	1813	Evaporator
CF_2	PCM_B	8.3	2235	Evaporator and lid
CF_3	PCM_B	6.8	1831	Evaporator
CF_4	PCM_B	1.5	404	Lid

Abbreviation: PCM, phase change material.

properties that were not originally provided by the manufacturer were derived using the similarity-weighted averaging approach described and added to Table 2.

No manufacturer was found providing values of thermal conductivity in the solid state and viscosity for PCMs with similar melting point, enthalpy of fusion, and density at the liquid phase to the values of PCM_A and PCM_B.

2.3 | Prototypes' Design and Manufacturing

Four unique prototypes were developed to investigate the benefits of integrating PCMs into domestic freezers by modifying the ordinary chest freezer described in Section 2.1. These modifications aimed to identify trends in how different strategies affect energy consumption and autonomy to electricity blackouts, with a view to both theoretical insights and actual commercialization.

The PCM-enhanced prototypes, labeled CF_1 to CF_4, contain different amounts of the PCMs described in Table 2, placed at the freezer's evaporator, top-mounted lid, or both locations. Table 5 summarizes the location, the mass employed, and the resultant extra storage capacity (kJ) for each prototype. The selection of the PCMs' mass values was grounded on the following criteria:

1. *Evaporator area coverage:* Ensuring that all the heat transfer area of the evaporator was fully covered without increasing the thickness of PCM slabs, thereby avoiding significant displacement of insulation.
2. *Door space utilization:* Maximizing the use of the available space in the interior part of the top-mounted door without

changing the original door design, which inevitably restricted the volume of PCM employed.

3. *Thermal energy storage:* Manufacturing prototypes with different values of additional thermal energy storage capacities within 200 and 2500 kJ, consistent with values employed by peers in previous studies on DRSs with PCMs [15, 19, 65–71].

The manufacturing process facilitated the PCM's integration, as these were assembled before the polyurethane injection process for insulation. For the CF_1 prototype, the eutectic gel (PCM_A) was manually encapsulated in polyethylene bags, which were then also manually placed in direct contact with the evaporator tube. This was eased by using an aluminum sheet (with 0.25 mm thickness) to improve thermal conductivity and ensure a uniform surface for insulation adherence. Figure 2 illustrates the outcome of this manual application process.

The polymeric bags were 55 mm wide, while their length depended on the dimensions of the walls on which they were applied. Aiming to cover all the available heat transfer areas of the evaporator, it was possible to apply 19 bags 405 mm long and 10 bags which were 660 mm long. For CF_1, by using PCM_A, each shorter bag encapsulated 0.175 kg of storage material, while the lengthier bags encapsulated 0.346 kg. Each PCM bag was sealed at the top and bottom, resulting in an enclosure that did not allow significant expansion of its volume in the third dimension. Hence, the adopted solution ensured that it was possible to minimize the amount of polyurethane foam displaced to accommodate the TES materials compared with the ordinary chest freezer CF_0.

By trapping the PCM bags near the evaporator with the polyurethane rigid foam for insulation ensured that theoretically the



FIGURE 2 | Pictures of the manual assembly of PCM_A to the evaporator of prototype CF_1. PCM, phase change material.

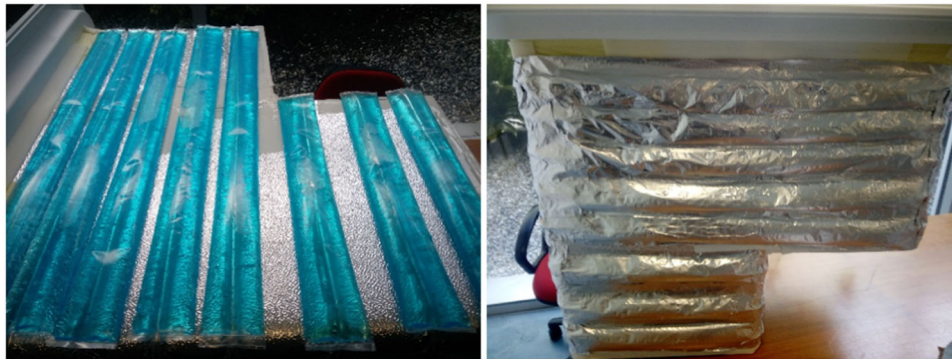


FIGURE 3 | Pictures of the manual application of PCM_B to the evaporator of prototype CF_2. PCM, phase change material.

thickness of the PCM units was the same as the evaporator tubes (6.8 mm). Thus, the 6.8 kg of PCM_A used in CF_1 was a result of maximizing the available space according to this methodology.

As the density of both PCMs is similar, the same methodology was replicated for CF_2, where we ensured that an equal mass of PCMs was used by manually encapsulating and laying 29 bags of PCM_B at the evaporator. Figure 3 clearly demonstrates a wall in which five bags are lengthier than the other three placed in contact with the evaporator tubes.

Additionally, we introduced an innovative design by developing a novel door for the freezer. The ordinary model featured a top-mounted lid that already included extra polyurethane thickness, surpassing the 90-mm insulation of the side walls (as mentioned in Table 1) to enhance thermal regulation and mitigate the additional heat gains through the door seal. Despite this extra insulation, the standard door also had free space on its interior side, consisting of a concavity, to ensure sufficient air clearance above the stored food contents.

So, for the novel door, we ensured the door retained the insulation thickness while filling this concavity with 1.5 kg of the PCM_B, as shown in Figure 4. This method leveraged a formerly unexploited space while saving the required air clearance, thus optimizing the freezer's design without compromising its net volume for food storage. Again, the criterion for determining the

mass of PCM_B was merely related to the maximization of the available space. As the available area was 0.298 mm^2 (423×705) and the maximum thickness possible to explore without compromising the required clearance to the foodstuff was 4.5 mm, approximately 1.5 kg was the maximum amount of PCM_B possible to apply.

The redesigned door was applied to both the CF_2 prototype, which featured PCM_B both at the evaporator and lid, and the CF_4 prototype. In CF_4, the focus was mainly on evaluating the door's impact, namely, to conclude how PCM affects the door insulation capability. Hence, we restricted modifications made to the original chest freezer to the application of this unique door while we ensured a prototype with less capacity to store energy and less displacement of insulation material.

For the development of the CF_3 prototype, we tested advancements in the manufacturing process, building on the insights from previous prototypes. This model maintained the same PCM mass employed at the evaporator used in CF_1 and CF_2 to enable direct comparisons. Yet, as shown in Figure 5, we engineered a strip of smaller polyethylene bags filled with PCMs, facilitating the simultaneous wrapping of the PCM bags and evaporator coil around the freezer compartment. This setup optimized thermal contact while ensuring even distribution along the walls. The assembly process was tested using an automated machine designed to uniformly wrap the evaporator

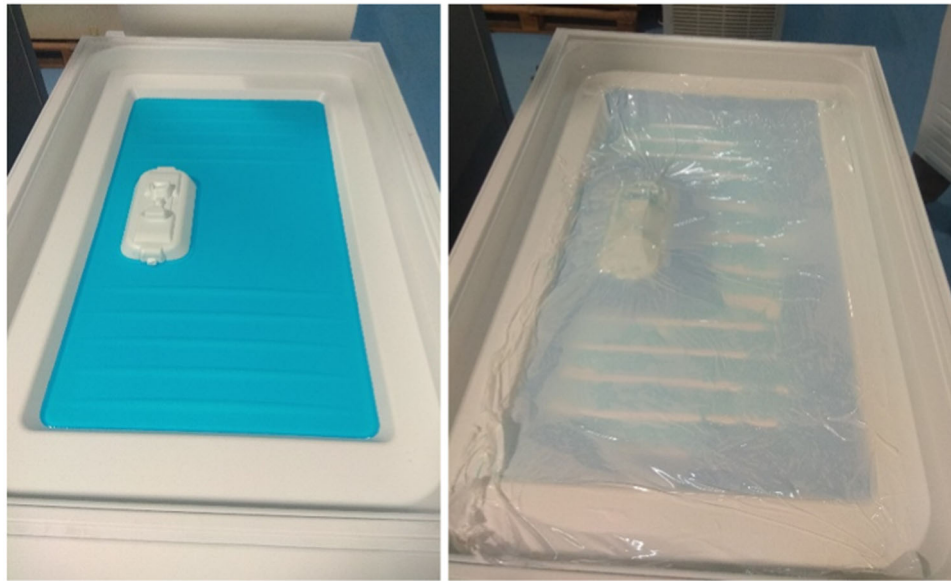


FIGURE 4 | Internal side of the freezer's lid after filling a previously free space with PCM_B. PCM, phase change material.

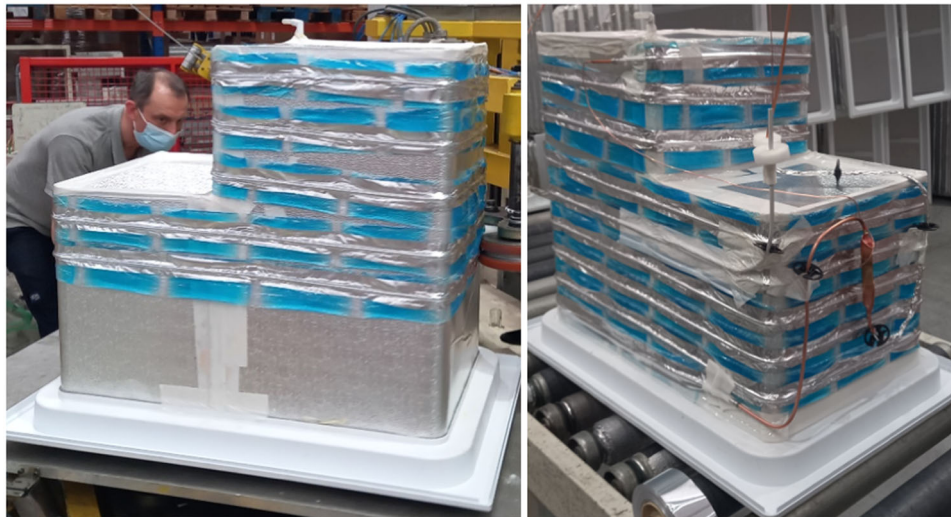


FIGURE 5 | Assembly of the CF_3 Prototype: Semiautomatic wrapping of the evaporator coil and PCM_B bags around the freezer compartment and final result before insulation foam injection.

along the freezers' walls and a human operator guiding the PCMs strip in alignment with the coil.

To address the thermal and volume expansion of the PCMs during use, careful consideration was given to their placement within the door and walls of the freezer. As shown in Figure 4, the plastic bags containing PCM would allow for expansion in the door. Moreover, we ensured that when the door is closed, the PCM can expand into the clearance space between the concavity of the door and the top layer of food contents or test packages. In the walls, each PCM bag was only filled to approximately 90% of its total capacity to allow for expansion, and the volume of injected polyurethane for insulation was slightly reduced compared with the original unit manufactured without PCMs. These adjustments provided the PCMs with space for expansion without compromising the systems' integrity.

In summary, after concluding all the manufacturing steps, including the injection of the polyurethane foam for the insulation, the PCM-enhanced prototypes held an arrangement of the PCM in different locations, which can be schematized as in Figure 6.

Regarding the cost of the PCM-enhanced chest freezers, the additional cost associated with the integration of PCMs was estimated based on the cost per kilogram of the TES materials [72, 73]. Considering the unit costs of 4.25€ for PCM_A and 3.90€ for PCM_B, respectively, the maximum total cost increase for each prototype compared with CF_0 was estimated as follows: 28.90 € for CF_1, 32.37€ for CF_2, 26.52€ for CF_3, and 5.85€ for CF_4. These cost increments are relatively minor when compared with the retail price of similar ordinary chest freezers without PCMs by TENSAL, which often vary from 200€ to 650€.

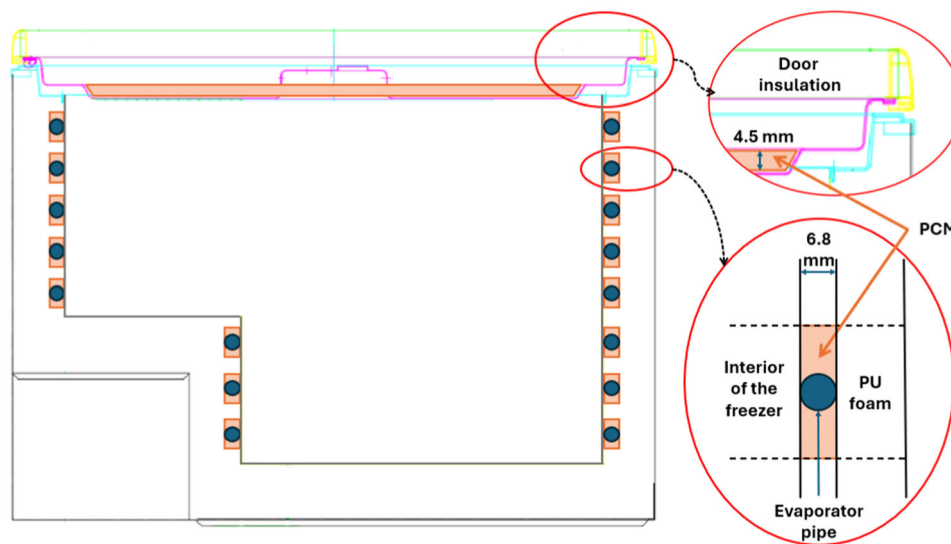


FIGURE 6 | Schematic of a cross-section of the freezer, including PCMs arrangement around the evaporator and in the door. PCM, phase change material; PU, polyurethane.



FIGURE 7 | Pictures of a freezing load test package (200 × 100 × 50) used inside the compartment.

2.4 | Test Provisions and Methodology

In this study, the test procedure respected, first and foremost, the requirements and test methods imposed by TENSAT Indústria, a specialized manufacturer of DRSS, which provided the test equipment and facilities. Their research and development efforts are focused on compliance with the standards that allow them to offer solutions with added commercial value.

The ordinary chest freezer without PCMs, described in Section 2.1 and hereby designated CF_0, along with the four PCM-enhanced prototypes (CF_1 to CF_4), was experimentally tested by adopting the test procedures established in the European Standard EN62552:2013. Each prototype was under investigation for two main test procedures: the temperature rise time test, which defines the freezer's autonomy, and the energy consumption test, which defines the daily energy consumption (kW.h/24 h).

This section details the experimental setup, equipment, and data collection methodology required to evaluate these technical specifications, which would feature on the product data-sheet if these systems were commercialized.

2.4.1 | Test Packages

For both test procedures conducted in this study, the European Standard adopted requires using test packages, as shown in Figure 7, placed inside the chest freezers' compartment. These packages replicate the thermal mass of food and were used in all our experiments. They comply with the rules established by the International Standard IEC 62552:2015, as well as its prior form, the original IEC 62552:2007, which was later slightly modified into the adopted EN 62552:2013.

Each package contains 230 g of oxyethylmethylcellulose, 764.2 g of water, 5 g of sodium chloride, and 0.8 g of 6-chloro-mcresol per kilogram. Their freezing point is -1°C , and the thermal attributes closely approximate those of lean beef, whose apparent specific heat capacity is described in [74]. Specifically, their specific heat capacity is described in the British Standard BS EN 161825:2016 as 2 ± 0.2 (kJ/(kg K)) and 3.7 ± 0.4 (kJ/(kg K)) at -30°C and $+20^{\circ}\text{C}$, respectively. Moreover, the specific enthalpy increases from -30°C to $+20^{\circ}\text{C}$ is 352 ± 7 (kJ/kg) [75, 76].

The standards also outline an alternative chemical composition for the test packages with $T_m = -5^{\circ}\text{C}$, which is only mandatory when conducting experiments in DRSS containing compartment

types other than freezers. So, for this study, we opted for the original formula with a higher melting point to prevent melting between test procedures, which could delay our experiments and increase the energy consumption for prefreezing the samples.

2.4.2 | Load Plan

After selecting the test packages, we ensured that our experimental setup complied with Clause 13 of EN 62552:2013. This clause defines that the freezer compartment shall be filled to maximum capacity with test packages while respecting the required top and side clearances, both for autonomy and energy consumption tests. Furthermore, it defines that the largest possible number of stacks of 1 kg packages (having a base of 100×200) must be used on the horizontal surfaces of the internal storage compartment and that the test packages of smaller dimensions must be used to complete the load plan, namely, at the top layers and at the thinner spaces.

Accordingly, a specific storage plan was predefined and tailored to the selected chest freezer model TCHEUSI180 by TENSAI Indústria. This plan included a total load of 119 kg, consisting of 149 test packages of varying dimensions and weights, spatially arranged as schematized in Figure 8.

For precisely monitoring temperature variations during testing, eight test packages were equipped with type-T thermocouples positioned at their geometrical centers. These packages, referred to as M-Packs, were labeled as S1–S8 in Figure 8. Their placement was based on guidelines from the European Standard,

which defines the test must monitor seven critical locations: the four corners and center at the top layer, the center of the bottom layer, and the area above the compressor step. Additionally, M-pack S3 was strategically placed at the geometric center of the compartment to enable systematic comparative analysis with the average temperature readings from the other seven M-packs. Table 6 details the characteristics of all test packages, categorized by size, quantity, and both individual and total weights.

2.4.3 | Temperature and Energy Consumption Measuring Equipment

For both the temperature rise time and energy consumption tests, data were recorded every 5 s, ensuring a high-resolution data set for detailed analysis. For collecting and recording the data, our setup was instrumented with sensors and acquisition modules for continuous monitoring and logging.

According to the load plan, temperature measurements were conducted using eight type-T thermocouples embedded within the M-packs to monitor temperature variations across different strategic regions of the freezer compartment. Each thermocouple was connected to a Yokogawa GX90 module, shown in Figure 9, for real-time data recording.

According to the general specifications, the Yokogawa GX90 module provides temperature measurement accuracy for type-T thermocouples of ±0.2°C for readings between 0°C and 400°C, and ±0.10% of the reading value +0.2°C for measurements in the range of −200°C to 0°C [77].

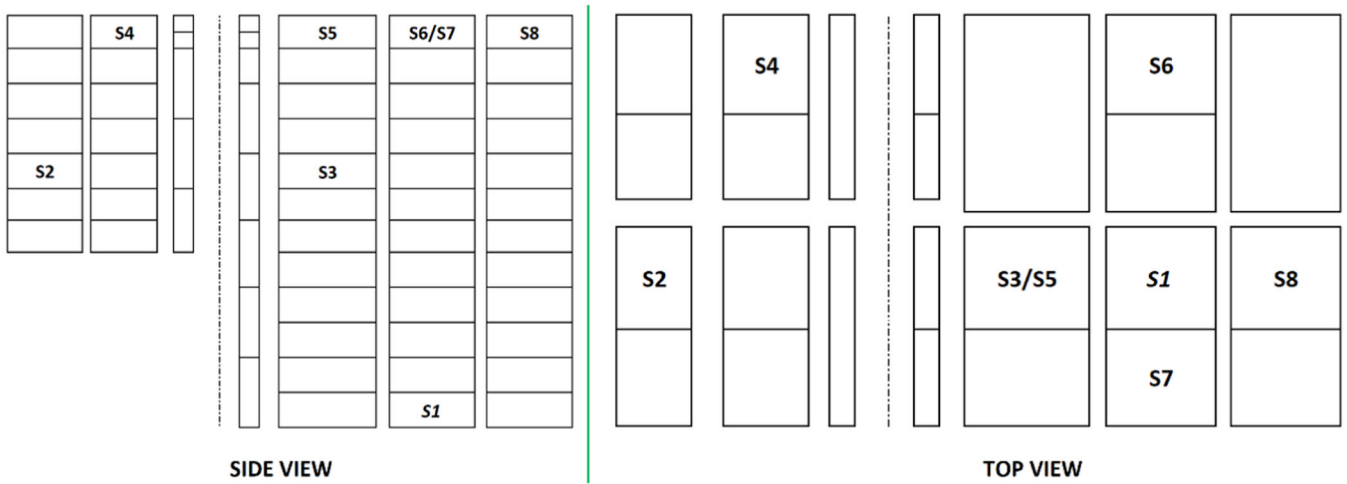


FIGURE 8 | Schematic of the load plan adopted for the experiments with standard test packages. (Left) Side view and (right) top view.

TABLE 6 | Characteristics of the test packages included in the load plan.

Package size (mm)	Number of packages	Weight per package (kg)	Total weight (kg)
25 × 50 × 100	16	0.125	2.0
50 × 50 × 100	4	0.250	1.0
50 × 100 × 100	26	0.500	13.0
50 × 100 × 200	103	1.00	103.0



FIGURE 9 | Yokogawa GX90 data acquisition module.



FIGURE 10 | Atto D4 RS485 230–240 V Transducer: Microprocessor-based energy analyzer for electrical data acquisition.

Electrical parameters, including current, voltage, power factor, frequency, and power consumption, were measured and recorded using the AttoD4 RS485 230–240 V transducer shown in Figure 10. This microprocessor-based energy analyzer facilitated precise electrical data acquisition across all test conditions.

According to the manufacturer's specifications, the Atto D4 transducer offers measurement accuracies of $\pm 0.5\%$ of the reading for both voltage and current, $\pm 0.02\text{Hz}$ for frequency, and $\pm 1\%$ of the reading for power measurements [78]. These values ensured reliable monitoring of electrical parameters, supporting detailed analysis of energy consumption and performance.

2.4.4 | Temperature Rise Time Test: Experimental Procedure

To assess the thermal resilience of our prototypes, the temperature rise time test was conducted in close adherence to Clause 16 of the European Standard, EN 62552:2013. This test assessed the thermal behavior of four-star freezer compartments under simulated power outage conditions, with the freezer compartment

fully loaded with test packages according to the load plan outlined in Section 2.4.2.

The experimental procedure began by precooling each prototype until all sensors (S1–S8) registered temperatures below -25°C , ensuring stabilized conditions at the mandatory room temperature per the standard of $+25^{\circ}\text{C}$. Once these conditions were achieved, the compressor was turned OFF, and data recording was started. Recordings of the eight temperature points were captured every 5 s until the first M-pack reached -9°C .

This procedure enabled measurement of the time interval from the instant when the first M-pack's temperature attained -18°C to the moment it rose to -9°C , a metric-denominated freezer's autonomy, indicating the duration over which the freezers maintain safe storage conditions during a power outage.

2.4.5 | Energy Consumption Test: Experimental Procedure

To optimize our method, the energy consumption tests, which establish the daily energy consumption for the technical data

sheet of DRSs, were conducted in each freezer immediately after conducting the autonomy test. So, each prototype (CF_0 to CF_4) remained fully loaded after the autonomy test, and the exterior ambient temperature was controlled at constant +25°C. This approach was based on a simplification of Clause 8 of IEC 62552:2007, which originally demanded testing class T freezers at +32°C of room temperature. The EN 62552:2013 modification enabled performing these tests at +25°C and with the same load plan [79–81].

Remarkably, we acknowledge that our energy consumption tests differ from the current version of IEC 62552:2015 in two respects: (1) it demands conducting energy consumption tests for two levels of ambient temperatures according to the freezers' climatic class (e.g., +16°C and +32°C) and (2) it states that the freezer compartments should be empty of test packages. Yet, when the model TCHEUSI180 of chest freezer was developed, the ruling standard, EN 62552:2013 (modified version of IEC 62552:2007), established per its Clause 15.2.2 that a load plan as the one described in Section 2.4.2 should be used.

Hence, our methodology enabled direct comparisons of the PCMs' impacts on energy consumption across prototypes (CF_1 to CF_4) tested under the same controlled and replicable conditions at which the ordinary chest freezer (CF_0) had been certified for market release.

The experimental procedure involved operating the freezers' compressor at a constant speed with the temperature control setting, that is, the thermostat governing the ON/OFF cycles, set to maintain average compartment temperature at or below −18°C. Tables 2 and 5 of EN 62552:2013 show that −18°C is the target storage temperature for four-star and three-star food freezer compartments. No defrost cycles were included in the test periods.

For each prototype, temperatures (S1–S8) and power consumption were recorded continuously for at least 24 h to capture complete temperature control cycles (ON/OFF) and account for the expected impact of the PCMs on both ON and OFF durations. This extended data collection ensured a long enough data set would be obtained for identifying a steady-state period of operation, as advised in Clauses 8.9 and 8.10 of EN 62552:2013, in which variations of storage temperatures and energy consumption values within 0.5 K and 3%, respectively, were found.

By adhering to these standard requirements, we ensured that data recording over a minimum 24-h test duration represented steady-state operation. Following an initial 24-h period of regular ON–OFF operation without data logging to achieve thermal stability, we recorded data on temperature and electrical parameters over a consistent steady-state period. Then, after selecting this stable period, the steady-state power (P) was calculated as the average of all measurements within that time-frame, and the daily energy consumption, E_{daily} , was calculated over exactly 24 h using Equation (1), expressed in kilowatt-hours per 24-h period (kW.h/24 h), as per the standard's requirements.

$$E_{\text{daily}} = P \times 24. \quad (1)$$

3 | Results and Discussion

This section presents results from the experimental tests performed on five prototypes of domestic chest freezers. Namely, we discuss the observed differences in temperature rise time, referred to as autonomy, and daily energy consumption across prototypes.

The temperature rise time test on the ordinary freezer provided valuable insights into temperature stratification inside the compartment. As expected, M-packs positioned at the bottom registered lower temperatures than those at the top due to the freezer's top-mounted door design. This temperature gradient was further exacerbated by heat gains through the door seal, which accelerated the heating of contents stored closer to the top of the compartment.

Figure 11 demonstrates this stratification, presenting the temperature rise curves for each M-pack (S1–S8) over 65 h, beginning from the moment each sensor recorded −25°C. Table 7 details the specific temperature reading observed at the various observation points after this time span.

These preliminary findings influenced our prototype development strategy, particularly in designing the novel door to stabilize temperatures at the top test packages. On the basis of these insights, we also decided to test the CF_4 prototype only for autonomy to evaluate the novel door's thermal performance.

Furthermore, our experimental results allowed us to evaluate the absolute temperature difference between the one measured at the geometric center of the freezers' compartments (measured by the purposely added S3 thermocouple) and the average temperature of the seven mandatory sensors. For each autonomy test (from CF_0 to CF_4), we calculated both the mean and maximum absolute differences after solving Equation (2) to each recorded value at 5-s intervals throughout the entire duration of each experimental procedure. Table 8 summarizes the results obtained.

$$\left| T_{S3} - \left(\frac{\sum_{i=1}^{n=8} T_{Si} - T_{S3}}{7} \right) \right|. \quad (2)$$

This analysis provided an estimate of how representative the temperature measurements at the geometric center of the compartment are in reflecting the average temperature distribution within it. These results are relevant for guiding future studies aiming to develop simplified numerical models to simulate different configurations of DRSs with PCMs tested for autonomy. For example, in the specific case investigated in this work, an ideal numerical model exactly simulating the temperature evolution of S3 under electricity blackout conditions would contain a maximum deviation of 4.14°C from the average of the seven mandatory M-packs per the EN62552:2013.

3.1 | Energy Autonomy

A systematic analysis of the results of temperature rise time tests revealed a consistent pattern across all prototypes: the

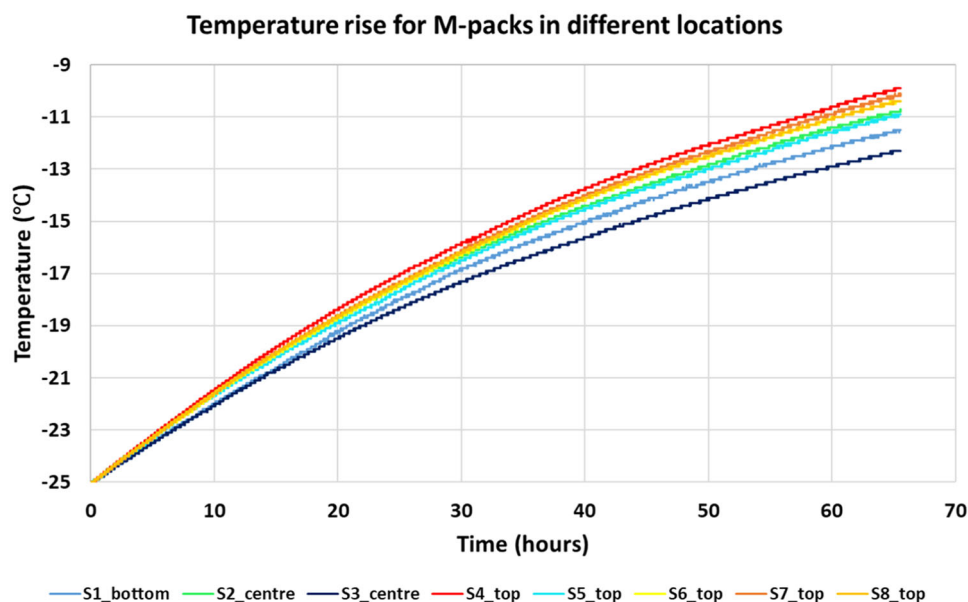


FIGURE 11 | Analysis of the temperature evolution of each M-pack inside the ordinary chest freezer following the load plan. Visualization of the 65 h after reaching -25°C for each temperature sensor.

TABLE 7 | Final temperatures of each M-pack of the load plan for the ordinary chest freezer, 65 h after reaching -25°C .

Sensor	S1	S2	S3	S4	S5	S6	S7	S8
Temperature 65 h after reaching -25°C	-11.5	-10.8	-12.3	-9.9	-10.9	-10.4	-10.1	-10.4

TABLE 8 | Analysis of the representativeness of measuring temperature at freezers' geometric center.

Prototype	Test Absolute differences ($^{\circ}\text{C}$)	Autonomy test	
		Mean	Maximum
CF_0		3.31	4.14
CF_1		2.90	3.44
CF_2		2.25	3.24
CF_3		2.43	3.28
CF_4		2.81	3.83

M-pack that first reached -18°C was also always the first to reach -9°C . Consequently, we isolated the data from the warmest M-pack in each freezer and normalized the time measurements starting when each respective sensor registered -25°C .

Table 9 presents the elapsed time for each prototype to reach the key temperatures of -18°C and -9°C . The time difference between hitting these two temperatures was calculated and rounded to the nearest integer, offering a clear measure of the autonomy extension achieved in prototypes CF_1 to CF_4 with PCMs compared with the conventional freezer without PCMs, which was labeled CF_0 for reference.

All prototypes demonstrated extended autonomy over the control unit, with CF_2 and CF_3 showing four times more resilience to power outages than CF_1 and CF_4. Specifically,

the temperature rise curves of the warmest M-packs, detailed in Figure 12, reveal that COOL -21°C PCM in CF_1 contributed to effectively stabilize temperatures in the early stages. In contrast, the equal mass of COOL -12°C PCM in CF_3 more effectively delayed temperature increases closer to the upper limit of -9°C .

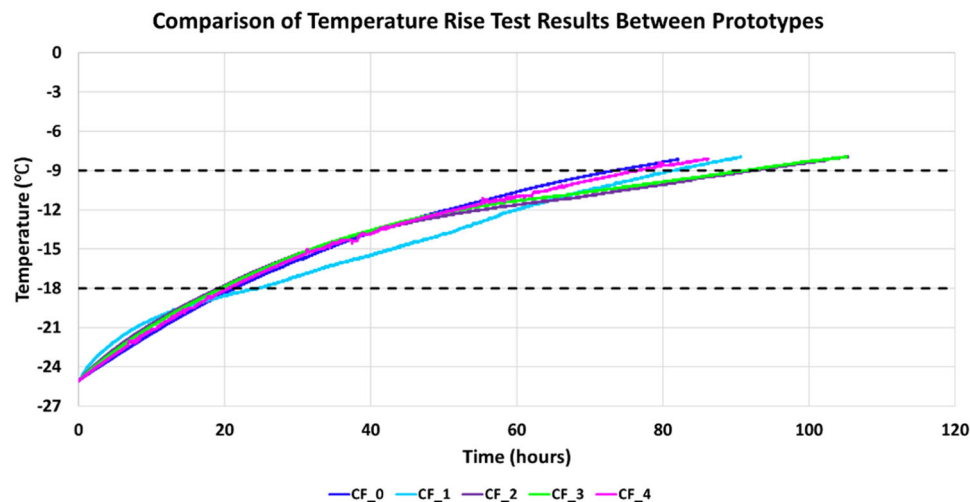
Despite adding similar latent heat storage capacities to CF_1 and CF_3 prototypes, the 9°C lower temperature gradient between the ambient temperature (25°C) and the melting points of the two PCMs (-21°C or -12°C) led to reduced heat gains in prototype CF_3. PCM_B melted more gradually, thereby extending autonomy more effectively.

The impact of the novel lid design was also evident in two ways. First, the door with the capacity to store 404 kJ was applied in CF_2 and contributed to an additional 2 h of autonomy compared with the CF_3 prototype. CF_3 held the same amount of PCMs in the walls as CF_2 but used the original door without PCMs. Second, the prototype CF_4, which differed from CF_0 only by the replacement of the original door with the innovative PCM-enhanced door containing 1.5 kg of PCM, demonstrated a 4-h increase the autonomy.

Our findings also revealed that while CF_4 had a significantly lower latent energy storage capacity of 404 kJ compared with the 1813 kJ of CF_1, both prototypes achieved similar enhancements in autonomy to power failures—4 and 5 h, respectively. This outcome is due to the 24% higher heat transfer rate observed in CF_1, as its PCM melts at a temperature 9°C lower than that of CF_4.

TABLE 9 | Data for determination of autonomy between -18°C and -9°C .

Prototype/data	CF_0	CF_1	CF_2	CF_3	CF_4
Time@ $T = -18^{\circ}\text{C}$ (h)	21.12	23.55	18.94	19.31	20.33
Time@ $T = -9^{\circ}\text{C}$ (h)	72.89	80.79	91.60	90.55	76.05
Autonomy (h)	52	57	73	71	56
Autonomy extension versus CF_0 (h)	0	+5	+21	+19	+4

**FIGURE 12** | Results of the temperature rise time tests for all prototypes with temperature evolution at the hottest M-packs.

Therefore, both CF_1 and CF_4 achieved comparable commercial attractiveness in terms of the datasheet specification of autonomy under failure despite being significantly different freezer designs. This underscores the importance of balancing PCM mass, selected melting point, and the extent of design modifications to optimize both performance and industrialization processes in novel freezers.

To support design decisions when advancing these prototypes to large-scale industrialization, the period factor analysis provides additional insights into the distinct commercial valuations. The period factor, defined in Equation (3), is the ratio between the time required for a specific location to reach a designated temperature (X) in a system with PCM integration versus without its use [82].

$$\text{period factor} = \frac{t_{\text{with/pcm@ } T = X^{\circ}\text{C}}}{t_{\text{no/pcm@ } T = X^{\circ}\text{C}}}. \quad (3)$$

Figure 13 presents the period factor calculated for our prototypes, tracking the time elapsed to reach each integer temperature value from -25°C to -9°C . A period factor above one indicates that PCM integration has delayed the temperature rise, thereby stabilizing food temperatures for longer. While all four PCM-enhanced chest freezers show a period factor above one at specific points, analyzing the entire range clarifies at which temperature, the rise rate slows down more effectively.

For instance, Figure 13 highlights that the CF_1 freezer is suitable for markets where power outages are brief and rare,

allowing the consumers to prioritize autonomy extension near the optimal storage temperature of -18°C . This effect results from the melting of the PCM used in CF_1, which occurs at -21°C and thus contributes to a period factor above one at lower temperatures, namely, from -18°C onwards.

In contrast, CF_2 and CF_3 prototypes are more appropriate choices for developing countries where electricity restoration may take days. These freezers provided nearly an additional day of autonomy by only achieving a period factor greater than one—that is, slowing the temperature rise—closer to the critical threshold of -9°C , making them particularly valuable in settings with prolonged power disruptions.

Hence, although CF_1 and CF_4 revealed 5 and 4 h of additional autonomy, respectively, the period factor analysis further clarified that their temperature stabilization occurs at significantly different temperatures across the tested range.

Finally, the period factor curve of CF_4 allowed us to assess the impact of incorporating PCMs in the door on its thermal insulation. Notably, the period factor remains slightly below 1 until the PCM starts to melt at -12°C , suggesting that the door's thermal conductivity was marginally reduced compared with CF_0. However, this minor loss in thermal insulation is offset by the benefits of the latent heat storage, as indicated by two indicators: Figure 13 reveals a period factor above 1 once the temperature surpasses -12°C for CF_4, and Table 9 highlights the addition of 4 h of autonomy.

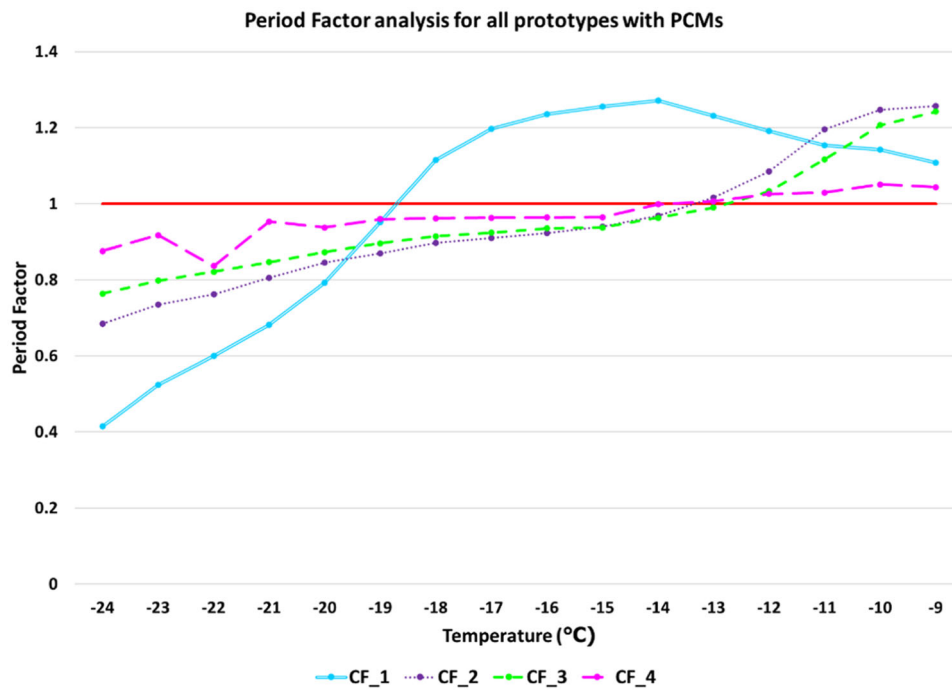


FIGURE 13 | Period factor comparison between prototypes with PCMs. PCM, phase change material.

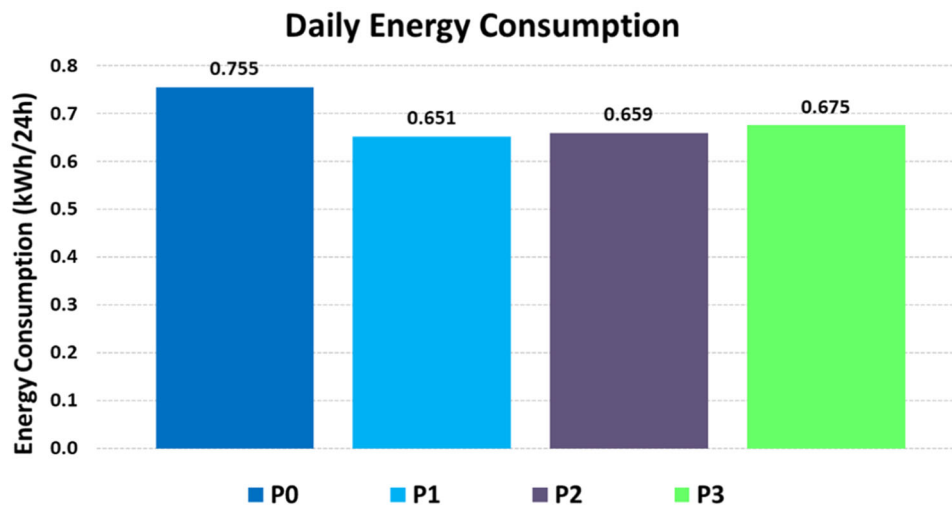


FIGURE 14 | Comparison of total daily energy consumption between prototypes.

3.2 | Energy Consumption

This section delves deeper into the impacts of integrating PCMs into domestic freezers. It presents the outcomes of the daily energy consumption tests. Our findings revealed notable savings in this metric amongst the prototypes equipped with PCMs.

Figure 14 presents a comparative overview, stressing that the PCM-enhanced prototypes achieved energy consumption reductions of up to 13% compared with the reference unit without PCMs. This reduction suggests that, despite an inevitable additional energy demand required to solidify the PCMs, the prototypes have the potential to meet or even exceed the current energy-efficiency labeling.

Despite the overall reductions, the daily energy consumption across prototypes CF_1 to CF_3 showed minimal variation, within a range of 4%. This similarity does not imply that the types, quantities, or locations of the PCMs had identical effects on system performance. Instead, as detailed below, distinct operational patterns of the compressor cycles emerged from each prototype. Specifically, Figure 15 details the 24-h energy consumption evolution, showing, for instance, that the CF_1 prototype with COOL -21°C (PCM_A), despite consuming more energy than CF_2 and CF_3, which included COOL -12°C (PCM_B), underwent fewer compressor cycles.

Hence, the prolonged ON and OFF times in the PCM-enhanced prototypes, as illustrated in Figure 15, resulted in different

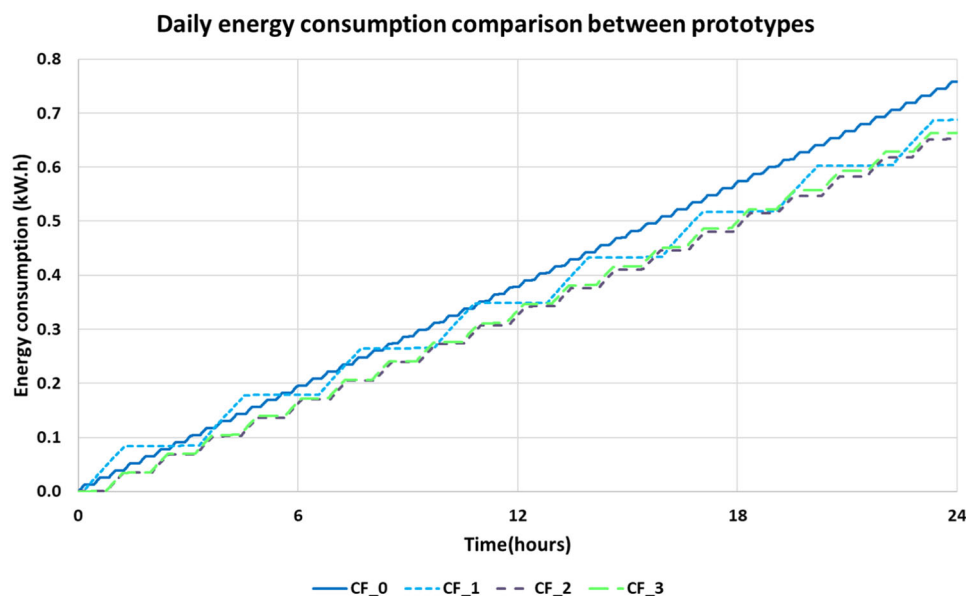


FIGURE 15 | Daily energy consumption evolution, including representation of each prototype's duty cycle (ON/OFF).

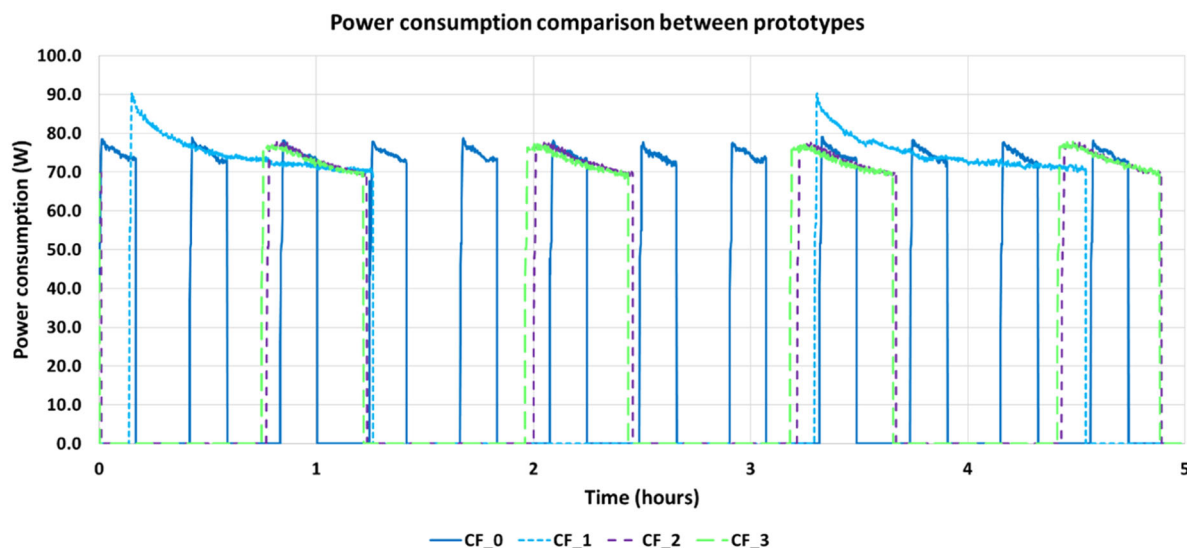


FIGURE 16 | Instantaneous power consumption evolution with each prototype's duty cycle (ON/OFF) representation.

compressor running time ratios. For reference, the CF_0 prototype without PCMs held a running time ratio of 42.0%, while the prototypes with PCMs showed ratios of 36.4% for CF_1, 38.4% for CF_2, and 38.5% for CF_3.

This analysis confirms that adding PCMs around the evaporator increases the load in the system, initially leading to an increase in the cooling time (compressor ON time) to reach the desired temperature before shutting OFF. Yet, this effect is positively offset by a significantly greater extension of the OFF times, thus resulting in overall energy savings across all PCM-enhance prototypes CF_1 to CF_3.

Interestingly, the instantaneous power demand profiles revealed that CF_2 and CF_3, using COOL -12°C (PCM_B),

closely matched those of the control unit, as shown in Figure 16. This was due to the use of PCMs that, during the energy consumption test, are completely solidified, thus not significantly affecting the heat transfer rate at the evaporator. The peak of instantaneous power demand was 79.9 W for the standard unit without PCMs, while for CF_2 and CF_3, it was 78.3 and 78.2 W, respectively.

Conversely, the CF_1 prototype showed the highest instantaneous compressor power demand of 90.4 W, revealing that while PCMs with lower melting points, closer to the freezer's setpoint, contribute to fewer compressor startups—potentially extending the units' lifetime—they also generate periods of more energy consumption demanding more electrical current.

In summary, our analysis of energy consumption and power demand patterns reveals unique trends in how the design choices impact each refrigeration system's energy efficiency and, consequently, their suitability for specific market needs. Specifically, CF_2 and CF_3 prototypes, which experience more frequent compressor startups than CF_1, revealed better suitability for regions with unstable power supplies, where their lower instantaneous power demands can help prevent grid overload and reduce blackout risks. In these markets, the CF_1 prototype would not be as appealing because its higher instantaneous power demand is more harmful to the context, and its potential benefits of autonomy extension are not even more significant than those of CF_2 and CF_3.

In contrast, in markets with robust electricity supply and rare power outages, users' trust in the electrical grid is much stronger, so solutions like the CF_1 prototype are more appealing. This is despite not saving as much energy, not finding as remarkable resilience to power outages, and not demanding low power values as CF_2 and CF_3. Instead, CF_1 finds a compromise between reducing energy consumption compared with CF_0 and offering a longer compressor lifespan supported by fewer compressor cycles, which are benefits most valued in these developed markets.

Such kinds of analysis highlights the advantages of testing PCM-enhanced refrigeration systems according to standardized protocols, facilitating credible and homogeneous comparisons that will be essential for scaling their commercialization and optimizing their suitability to market specifics.

Hence, we advocate for further enduring these discussions in future studies, namely, exploring the application of the most recent version of the international standard widely recognized, the IEC 62552-2:2015/AMD1:2020 and to different types of DRSs. Preferably, while overcoming a limitation observed in the EN 62552:2013 and IEC 62552:2015 standards that our methodology also contained, related to not closely monitoring the PCMs' temperature by affecting a specific thermocouple.

During the energy consumption tests presented in this paper, the thermostat ensured the freezer contents remained below the -18°C target, meaning that PCM_B ($T_m = -12^{\circ}\text{C}$) used in CF_2 and CF_3 was unlikely changing from the solid state. In contrast, PCM_A used in CF_1 melting at $T_m = -21^{\circ}\text{C}$, which is a closer temperature to the ones recorded in the M-packs, led to higher power demands, suggesting partial phase changes. Yet, this was not confirmed through the lack of dedicated sensors for measuring PCM's temperature.

Future studies and future versions of the international standards should thus account for the possibility of employing different control strategies considering based on the real-time monitoring of the PCMs' state of charge (liquid fraction) at the energy consumption test procedure that defines the final technical datasheet specifications. Namely, this will help clarify if further energy savings are possible with each configuration of PCM-enhanced DRS.

3.3 | Error and Uncertainty Analysis

As discussed in Section 2.4.3, the accuracy limitations of the temperature and power measurement equipment introduce an inherent uncertainty in the recorded values. To quantify this, the absolute uncertainty in temperature readings was calculated for the warmer M-pack across all tested prototypes. Since all temperature readings during the temperature rise tests fell within the range of -200°C to 0°C , the corresponding measurement error was determined using the manufacturer-specific accuracy of $\pm 0.10\%$ of the reading plus 0.2°C . This resulted in an average absolute error of 0.215°C and a maximum absolute error of 0.235°C .

Regarding power consumption, the absolute error in the power readings recorded at 5-s intervals was evaluated based on the equipment's expected accuracy of $\pm 1\%$. This analysis yielded an average absolute error of 0.286 W , and a maximum absolute error of 0.904 W was registered.

Since both temperature and power measurements had associated uncertainties, the results presented above for autonomy and energy consumption can be interpreted as intervals rather than exact values. Specifically, by propagating these measurement errors, the lower and upper bounds for the estimated autonomy and daily energy consumption of all prototypes are presented in Table 10. From this analysis, it is concluded that the autonomy extension and energy consumption reductions obtained by the PCM-enhanced chest freezers may, in reality, fall in an interval of values.

While the values reported in Sections 3.1 and 3.2 provide reliable estimates of each prototype's performance, namely, in Table 9 and Figure 14, minor deviations may occur due to the measurement uncertainties. To further illustrate this variability, Table 11 presents the possible range of autonomy extension and daily energy consumption reductions for each prototype, relative to the reference CF_0.

This analysis highlights that the estimated autonomy and energy consumption of the PCM-enhanced freezers are subject to measurement uncertainty, leading to variations in the reported values. Despite these uncertainties, the findings confirm that the studied configurations for PCM

TABLE 10 | Estimated autonomy and daily energy consumption across prototypes considering measurement-associated errors.

Prototype/ test	Autonomy (h)		Daily energy consumption (kW.h/24 h)	
	Lower bound	Upper bound	Lower bound	Upper bound
CF_0	50.50	53.06	0.747	0.762
CF_1	55.55	56.98	0.645	0.658
CF_2	71.00	74.27	0.652	0.665
CF_3	69.17	72.96	0.668	0.681
CF_4	54.68	56.78	—	—

TABLE 11 | Range of autonomy and energy consumption variations relative to CF_0.

Prototype	Autonomy variation compared with CF_0 (h)		Daily energy consumption variation compared with CF_0 (kW.h/24 h)	
	Minimum	Maximum	Minimum	Maximum
CF_1	+2.49	+6.48	−0.089	−0.117
CF_2	+17.94	+23.77	−0.082	−0.110
CF_3	+16.11	+22.46	−0.066	−0.094
CF_4	+1.62	+6.28	—	—

integration would always enhance the freezer's autonomy and reduce energy consumption, under the standardized testing characteristics, reinforcing the potential of this technology for commercial applications.

Since the present uncertainty analysis is based on instrumental errors only and does not account for statistical variability, future studies could refine these estimates by:

- Conducting repeatability tests to assess experimental variability beyond sensor accuracy and quantify statistical uncertainty.
- Performing long-term aging studies to evaluate the impact of PCM degradation on the freezer performance over time.
- Incorporating sensitivity analyses to determine how specific parameters (e.g., ambient temperature fluctuations) influence freezers' performance.

4 | Conclusions

This research illustrates the advantages of integrating PCMs into DRSs, such as reducing energy consumption and extending autonomy during power outages. Developing and testing four innovative chest freezers has contributed to advancing the focus from proof-of-concept purposes to large-scale industrialization goals, providing relevant information towards the commercialization of market-oriented solutions.

The study introduces a novel, top-mounted lid containing PCMs and an innovative technique for automatically wrapping the evaporator coil and PCM bags. These were tested in manufacturing to enhance the freezers' performance without compromising food storage capacity.

Our methodology fills a gap in the literature as we experimentally tested the prototypes in close adherence to the European Standard EN 62552:2013. That allowed us to compare prototypes based on internationally recognized metrics derived from standards widely adopted by industrial manufacturers, which highlights the applied nature of this research work. Specifically, our findings of up to 40% of additional resilience to electricity blackouts are based on analyzing the temperature rise time test results within a normative but typically overlooked interval for frozen food preservation from -18°C to -9°C .

In summary, we observed that a simply manufactured top-lid with PCMs provided 4 h of additional autonomy, while a more

complex freezer requiring innovation in the assembly methodology to place the PCMs around the compartment resulted in similar five extra hours of blackout resilience. Yet, their diverse capacities to store energy—404 kJ versus 1813 kJ, respectively—make them tailored to different markets considering regional contexts and consumer needs. Specifically, in sophisticated markets, customers are more willing to bear the expected monetary, resource, and time costs associated with the more complex solution to benefit from greater thermal energy storage potential likely to store renewable energy.

Furthermore, the period factor analysis strengthens the practical impact of our research to empower industrialization and design decision-making towards commercialization. Namely, it highlights the market value of different PCMs' selection and application strategies. It suggests favouring higher melting points for regions where electricity restoration may take days and lower melting temperatures for markets prioritizing autonomy gains near-optimal storage temperature.

Notwithstanding our contributions, the study was limited by the inability to test the novel door with COOL -21°C PCM since it would not completely freeze within our test procedures and by the minor deviations from the current guidelines of the IEC 62552:2015 and EN 62552:2020 during energy consumption testing. Hence, future research should explore varying PCMs' melting temperatures in similar lids and conduct energy consumption tests in fully unloaded freezers to validate similar trends of energy consumption savings demonstrated by our estimations of up to 13% reductions. Other standardized testing procedures, such as the pull-down test, should also be conducted in PCM-enhanced prototypes.

While this study provides valuable insights into the effects of PCM quantity and melting temperature on system performance, a comprehensive characterization of PCM thermophysical properties was beyond the scope of this work. The presented values estimated through a similarity-weighted averaging approach must be confirmed in future studies, while the characterization must also aim at studying solid-state thermal conductivity and viscosity.

Further investigation should also systematically evaluate the impacts of varying these properties under controlled conditions to further enhance our understanding of their role in PCM-enhanced refrigeration systems' transient thermal response and energy performance.

Moreover, the expected useful life of PCM-enhanced freezers is anticipated to be comparable to that of conventional freezers

currently available in the market, provided that no unexpected corrosion or leakage issues emerge from the PCM's units. In any case, future studies are required to assess the long-term stability and determine whether the performance gains of the PCM-enhanced chest freezers remain true after extensive thermal cycling of the PCMs, including hundreds or thousands of phase changes.

While the general potential for energy consumption reduction and autonomy extension observed in this study is likely relevant and achievable in other DRS types, further research is needed to evaluate different refrigeration systems with other compartment types under the standardized test procedures outlined in international standards. For instance, the exact autonomy extension values measured in hours for our chest freezers based on a given criterion are not representative of what values could be expected in fresh-food compartments. Notably because current standards lack a uniform criterion for assessing autonomy in fresh-food compartments, such as a temperature interval from 2°C to 8°C, which would support similar studies to the one in this paper but not on refrigerators without freezer compartments. Such studies may include a comparison between the European Standard EN62552:2013 and those from different world regions, such as the Colombian Technical Standard NTC5891 or the Iranian ISIRI 13700, hereby mentioned in the literature review as already adopted by peer-researchers.

Nomenclature

Math Formulations, Subscripts, and Greek Symbols

$$\text{Cycle}_{\text{time}} = \text{ON}_{\text{time}} + \text{OFF}_{\text{time}}$$

$$E_{\text{daily}} = P \times 24 - \text{Daily energy consumption}$$

$$\text{period factor} = \frac{t_{\text{with/pcm@ } T=X^{\circ}\text{C}}}{t_{\text{no/pcm@ } T=X^{\circ}\text{C}}}$$

$$\text{Running time} = \frac{\text{ON}_{\text{time}}}{\text{Cycle}_{\text{time}}}$$

$$T_m \text{ melting temperature}$$

Units

Daily energy consumption kW.h/24 h

Density kg/m³

Enthalpy of fusion – Latent heat kJ/kg

Power W

Temperature °C

Time h

Author Contributions

Daniel Marques: conceptualization, methodology, investigation, writing – original draft preparation, data curation, formal analysis, writing – reviewing and editing. **Vitor Silva:** conceptualization, investigation, methodology, resources, supervision, validation, writing – reviewing and editing. **Nelson Martins:** resources, supervision, writing – reviewing and editing, project administration, funding acquisition. **Fernando Neto:** resources, supervision, writing – reviewing and editing, project administration, funding acquisition.

Acknowledgments

The authors acknowledge the Fundação para a Ciência e a Tecnologia (FCT), Portugal, for supporting the PhD Grant Scholarship, grant reference 2021.06083.BD, and all the staff working at the Centre for Mechanical Technology and Automation, University of Aveiro, and Tensai Indústria, SA. This work was supported by the Fundação para a Ciência e a Tecnologia (FCT), the Portuguese National Foundation for Science and Technology (grant number 2021.06083.BD) and by the projects UIDB/00481/2020 and UIDP/00481/2020—Fundação para a Ciência e a Tecnologia, DOI 10.54499/UIDB/00481/2020 (<https://doi.org/10.54499/UIDB/00481/2020>) and DOI 10.54499/UIDP/00481/2020 (<https://doi.org/10.54499/UIDP/00481/2020>), and CENTRO-01 0145-FEDER-022083 under the program “Centro Portugal Regional” (Centro2020), and the PORTUGAL 2020 partnership agreement, through the European Regional Development Fund.

Conflicts of Interest

The authors declare no conflicts of interest.

Data Availability Statement

The authors have nothing to report.

References

1. J. M. Belman-Flores, J. M. Barroso-Maldonado, A. P. Rodríguez-Muñoz, and G. Camacho-Vázquez, “Enhancements in Domestic Refrigeration, Approaching a Sustainable Refrigerator—A Review,” *Renewable and Sustainable Energy Reviews* 51 (2015): 955–968, <https://doi.org/10.1016/j.rser.2015.07.003>.
2. J.-L. Dupont, P. Domanski, P. Lebrun, and F. Ziegler, “New IIR Informatory Note on the Role of Refrigeration in the Global Economy,” in *38th IIR Informatory Note the Role of Refrigeration in the Global Economy Published in June 2019* (International Institute of Refrigeration, 2019), <https://iifir.org/en/news/new-iir-informatory-note-on-the-role-of-refrigeration-in-the-global-economy-ba8bd933-a1dd-4710-a4ef-9794ec0c063d>.
3. J.-L. Dupont, “The Role of Refrigeration in the Global Economy,” in *38th Note on Refrigeration Technologies* (International Institute of Refrigeration, 2019), <https://doi.org/10.18462/iif.NItc38.06.2019>.
4. T. H. Meles, “Impact of Power Outages on Households in Developing Countries: Evidence From Ethiopia,” *Energy Economics* 91 (2020): 104882, <https://doi.org/10.1016/j.eneco.2020.104882>.
5. M. A. Cole, R. J. R. Elliott, G. Occhiali, and E. Strobl, “Power Outages and Firm Performance in Sub-Saharan Africa,” *Journal of Development Economics* 134 (2018): 150–159, <https://doi.org/10.1016/j.jdevco.2018.05.003>.
6. InsightAce Analytic, *Vaccine Cold Chain Logistics Market Expected to Reach US\$ 4.90 Billion by 2030—Growing Beyond COVID-19 Application* (2022), accessed December 13, 2022, <https://www.prnewswire.com/news-releases/vaccine-cold-chain-logistics-market-expected-to-reach-us-4-90-billion-by-2030—growing-beyond-covid-19-application-301686152.html>.
7. Grand View Research, *Cold Chain Market Size & Growth Report, 2021–2028* (2021), accessed December 13, 2022, <https://www.grandviewresearch.com/industry-analysis/cold-chain-market>.
8. C. James, B. A. Onarinde, and S. J. James, “The Use and Performance of Household Refrigerators: A Review,” *Comprehensive Reviews in Food Science and Food Safety* 16 (2017): 160–179, <https://doi.org/10.1111/1541-4337.12242>.
9. Insight Ace Analytic, *Cold Chain Logistics Market* (2022), accessed December 13, 2022, <https://www.insightaceanalytic.com/report/global-vaccine-cold-chain-logistics-market/1127>.
10. H. Selvnnes, Y. Allouche, R. I. Manescu, and A. Hafner, “Review on Cold Thermal Energy Storage Applied to Refrigeration Systems Using

- Phase Change Materials," *Thermal Science and Engineering Progress* 22 (2021): 100807, <https://doi.org/10.1016/j.tsep.2020.100807>.
11. A. Sharma, V. V. Tyagi, C. R. Chen, and D. Buddhi, "Review on Thermal Energy Storage With Phase Change Materials and Applications," *Renewable and Sustainable Energy Reviews* 13 (2009): 318–345, <https://doi.org/10.1016/j.rser.2007.10.005>.
 12. B. Kiran-Yildirim, "Performance Evaluation of a Laboratory-Scale Cooling System as a Household Refrigerator With Phase Change Materials," *Energy Sources, Part A: Recovery, Utilization, and Environmental Effects* 44 (2022): 5852–5867, <https://doi.org/10.1080/15567036.2022.2089300>.
 13. J. Riffat, C. Kutlu, E. Tapia-Brito, et al., "Development and Testing of a PCM Enhanced Domestic Refrigerator With Use of Miniature DC Compressor for Weak/Off Grid Locations," *International Journal of Green Energy* 19 (2022): 1118–1131, <https://doi.org/10.1080/15435075.2021.1984244>.
 14. Z. Liu, D. Zhao, Q. Wang, Y. Chi, and L. Zhang, "Performance Study on Air-Cooled Household Refrigerator With Cold Storage Phase Change Materials," *International Journal of Refrigeration* 79 (2017): 130–142, <https://doi.org/10.1016/J.IJREFRIG.2017.04.009>.
 15. M. Antony Forster Raj and S. Joseph Sekhar, "Investigation of Energy and Exergy Performance on a Small-Scale Refrigeration System With PCMs Inserted Between Coil and Wall of the Evaporator Cabin," *Journal of Thermal Analysis and Calorimetry* 136 (2019): 355–365, <https://doi.org/10.1007/s10973-018-7785-7>.
 16. G. Sonnenrein, E. Baumhögger, A. Elsner, et al., "Improving the Performance of Household Refrigerating Appliances Through the Integration of Phase Change Materials in the Context of the New Global Refrigerator Standard IEC 62552:2015," *International Journal of Refrigeration* 119 (2020): 448–456, <https://doi.org/10.1016/j.ijrefrig.2020.07.025>.
 17. A. Husainy, S. Sawant, S. Kale, and S. Nishandar, "Experimental Investigation of Eutectic Phase Changing Materials (KCl + Na₂SO₄) Mixed With Graphene (Gr) Nano-Particles on Refrigeration Test Rig," *Materials Today: Proceedings* 72 (2023): 1510–1516, <https://doi.org/10.1016/J.MATPR.2022.09.379>.
 18. T. B. Radebe, A. U. C. Ndanduleni, and Z. Huan, "Investigation of Low-Cost Eutectic Salts to Ensure Food Products During Power Outages," *Journal of Energy Storage* 63 (2023): 106960, <https://doi.org/10.1016/J.EST.2023.106960>.
 19. E. Oró, L. Miró, M. M. Farid, and L. F. Cabeza, "Improving Thermal Performance of Freezers Using Phase Change Materials," *International Journal of Refrigeration* 35 (2012): 984–991, <https://doi.org/10.1016/j.ijrefrig.2012.01.004>.
 20. E. Oró, L. Miró, M. M. Farid, and L. F. Cabeza, "Thermal Analysis of a Low Temperature Storage Unit Using Phase Change Materials Without Refrigeration System," *International Journal of Refrigeration* 35 (2012): 1709–1714, <https://doi.org/10.1016/j.ijrefrig.2012.05.004>.
 21. L. N. Mane and P. A. Patil, "Experimental Investigation of the Effect of Phase Change Material on Backup Time and Equivalent Energy Consumption of Domestic Refrigerator," *Energy Storage and Saving* 3 (2024): 250–258, <https://doi.org/10.1016/J.ENSS.2024.07.001>.
 22. Y. Yusufoglu, T. Apaydin, S. Yilmaz, and H. O. Paksoy, "Improving Performance of Household Refrigerators by Incorporating Phase Change Materials," *International Journal of Refrigeration* 57 (2015): 173–185, <https://doi.org/10.1016/j.ijrefrig.2015.04.020>.
 23. M. I. H. Khan and H. M. M. Afroz, "Experimental Investigation of Performance Improvement of Household Refrigerator Using Phase Change Material," *International Journal of Air-Conditioning and Refrigeration* 21 (2013): 1350029, <https://doi.org/10.1142/S2010132513500296>.
 24. M. I. H. Khan and H. M. M. Afroz, "Effect of Phase Change Material on Compressor On–Off Cycling of a Household Refrigerator," *Science and Technology for the Built Environment* 21 (2015): 462–468, <https://doi.org/10.1080/23744731.2015.1023161>.
 25. J. Cofré-Toledo, D. A. Vasco, C. A. Isaza-Roldán, and J. A. Tangarife, "Evaluation of an Integrated Household Refrigerator Evaporator With Two Eutectic Phase-Change Materials," *International Journal of Refrigeration* 93 (2018): 29–37, <https://doi.org/10.1016/j.ijrefrig.2018.06.003>.
 26. M. S. Padhye and N. Agrawal, "Integration of Phase Change Materials (PCMs) in Freezer of a Domestic Refrigerator: A Comparative Study," *Journal of the Institution of Engineers (India): Series C* 104 (2023): 1057–1064, <https://doi.org/10.1007/s40032-023-00972-7>.
 27. M. Rahimi, A. A. Ranjbar, and M. J. Hosseini, "Experimental Investigation on PCM/Fin Slab Incorporation in a Evaporator Side of a Household Refrigerator," *Energy Reports* 10 (2023): 407–418, <https://doi.org/10.1016/j.egyr.2023.06.053>.
 28. L. Abdolmaleki, S. M. Sadrameli, and A. Pirvaram, "Application of Environmental Friendly and Eutectic Phase Change Materials for the Efficiency Enhancement of Household Freezers," *Renewable Energy* 145 (2020): 233–241, <https://doi.org/10.1016/j.renene.2019.06.035>.
 29. S. Joseph Sekhar, F. Saif Al Maqbali, and J. Aslam, "Phase Change Materials (PCM) for a Zero-Carbon Food Preservation Technology in Remote Areas," *IOP Conference Series: Earth and Environmental Science* 1365 (2024): 012009, <https://doi.org/10.1088/1755-1315/1365/1/012009>.
 30. M. R. Jasim, H. S. Sultan, and F. A. Abood, "Experimental Investigation of the Performance of a Household Refrigerator Using Phase Change Material," *Basrah Journal for Engineering Science* 23 (2023): 99–107.
 31. D. V. A. Pharande and S. A. Desai, "A Performance Enhancement of Household Refrigerator Using Phase Change Materials (PCMs)," *International Journal of Scientific Research in Engineering and Management* 9, no. 5 (2023): 2185–2189, <https://doi.org/10.55041/IJSREM18384>.
 32. A. Pirvaram, S. M. Sadrameli, and L. Abdolmaleki, "Optimization of Energy Consumption and Temperature Fluctuations for a Household Freezer Using Non-Toxic and Non-Flammable Eutectic Phase Change Materials With a Cascade Arrangement," *International Journal of Energy Research* 45 (2021): 1775–1788, <https://doi.org/10.1002/er.5853>.
 33. Technical Committee T 59/SC 59M, *IEC 62552-1 Consolidated Version—IEC 62552-1:2015+AMD1:2020 CSV | IEC Webstore—Household Refrigerating Appliances—Characteristics and Test Methods—Part 1: General Requirements, International Standard* (2020), accessed October 13, 2023, <https://webstore.iec.ch/publication/68114>.
 34. Technical Committee T 59/SC 59M, *IEC 62552-1 Consolidated Version—IEC 62552-2:2015+AMD1:2020 CSV | IEC Webstore—Household Refrigerating Appliances—Characteristics and Test Methods—Part 2: Performance Requirements, International Standard* (2020), accessed October 13, 2023, <https://webstore.iec.ch/publication/68116>.
 35. Technical Committee T 59/SC 59M, *IEC 62552-1 Consolidated Version—IEC 62552-3:2015+AMD1:2020 CSV | IEC Webstore—Household Refrigerating Appliances—Characteristics and Test Methods—Part 3: Energy Consumption and Volume, International Standard* (2020), accessed October 13, 2023, <https://webstore.iec.ch/publication/68117>.
 36. Technical Committee C 59X, *EN 62552:2013—Household Refrigerating Appliances—Characteristics and Test Methods, European Standard* (2013), accessed July 24, 2024, <https://standards.iteh.ai/catalog/standards/clc/19cf1403-1cc7-4eff-83a3-f61698764410/en-62552-2013>.
 37. Technical Committee F, *SIST EN 62552:2013—Household Refrigerating Appliances—Characteristics and Test Methods (IEC), European Standard* (2013), accessed July 24, 2024, <https://standards.iteh.ai/catalog/standards/sist/4aad3a5a-5ed8-4eab-a712-cca88d295650/sist-en-62552-2013>.
 38. European Committee for Standards—Electrical, *EN 62552:2013 Household Refrigerating Appliances—Characteristics and Test Methods, European Standard* (2013), accessed July 24, 2024, https://shop.standards.ie/en-ie/standards/en-62552-2013-352101_saig_cenelec_cenelec_803515/.

39. TENSAT Indústrias, *TCHEUSI180—Tensai* (2024), accessed April 3, 2024, <https://www.tensai.pt/domestico/congeladores-horizontais/tcheusi180/>.
40. TENSAT Indústrias, *Ficha TCHEUSI180.pdf—Google Drive* (2024), accessed April 3, 2024, <https://drive.google.com/file/d/1DRBx0H23FaIkfbv8dZCbW-rTjEjBXrn/view>.
41. Secop, *Product Details Secop Compressor BD80CN | Secop* (2024), accessed April 3, 2024, <https://selector.secop.com/application-search/variants/101Z0403/>.
42. Secop, *BD80CN Direct Current Compressor R290, 12/24V DC, 10-45V DC Solar & 100-240V AC 50/60Hz* (2024), accessed April 3, 2024, https://www.secop.com/fileadmin/user_upload/SEPS/datasheets/en/bd80cn_101z0403_r290_12-24vdc_01-2024_desd100r902.pdf.
43. Y. Phimolsiripol, U. Siripatrawan, V. Tulyathan, and D. J. Cleland, "Effects of Freezing and Temperature Fluctuations During Frozen Storage on Frozen Dough and Bread Quality," *Journal of Food Engineering* 84 (2008): 48–56, <https://doi.org/10.1016/j.jfoodeng.2007.04.016>.
44. J. Y. Sze, C. Mu, A. Romagnoli, and Y. Li, "Non-Eutectic Phase Change Materials for Cold Thermal Energy Storage," *Energy Procedia* 143 (2017): 656–661, <https://doi.org/10.1016/J.EGYPRO.2017.12.742>.
45. P. Boutron, A. Kaufmann, and N. Van Dang, "Maximum in the Stability of the Amorphous State in the System Water–Glycerol–Ethanol," *Cryobiology* 16 (1979): 372–389, [https://doi.org/10.1016/0011-2240\(79\)90050-6](https://doi.org/10.1016/0011-2240(79)90050-6).
46. J. Liesebach, M. Lim, and T. Rades, "Determination of Unfrozen Matrix Concentrations at Low Temperatures Using Stepwise DSC," *Thermochimica Acta* 411 (2004): 43–51, <https://doi.org/10.1016/J.TCA.2003.07.005>.
47. A. Ghodrati, R. Zahedi, and A. Ahmadi, "Analysis of Cold Thermal Energy Storage Using Phase Change Materials in Freezers," *Journal of Energy Storage* 51 (2022): 104433, <https://doi.org/10.1016/j.est.2022.104433>.
48. T. Zhang, T. Li, E. Nies, H. Berghmans, and L. Ge, "Isothermal Crystallization Study on Aqueous Solution of Poly(Vinyl Methyl Ether) by DSC Method," *Polymer* 50 (2009): 1206–1213, <https://doi.org/10.1016/J.POLYMER.2008.12.038>.
49. Y. Ying, Y. Hongyuan, and S. Haiying, "Development of a Low Temperature Phase Transforming Composed Material for Cool Storage," *Journal of Superconductivity and Novel Magnetism* 23 (2010): 1115–1117, <https://doi.org/10.1007/s10948-010-0650-y>.
50. A. A. M. Omara and A. A. M. Mohammedali, "Thermal Management and Performance Enhancement of Domestic Refrigerators and Freezers via Phase Change Materials: A Review," *Innovative Food Science & Emerging Technologies* 66 (2020): 102522, <https://doi.org/10.1016/J.IFSET.2020.102522>.
51. E. Oró, A. de Gracia, A. Castell, M. M. Farid, and L. F. Cabeza, "Review on Phase Change Materials (PCMs) for Cold Thermal Energy Storage Applications," *Applied Energy* 99 (2012): 513–533, <https://doi.org/10.1016/j.apenergy.2012.03.058>.
52. G. Li, Y. Hwang, R. Radermacher, and H. H. Chun, "Review of Cold Storage Materials for Subzero Applications," *Energy* 51 (2013): 1–17, <https://doi.org/10.1016/J.ENERGY.2012.12.002>.
53. M. Mastani Joybari, F. Haghighat, J. Moffat, and P. Sra, "Heat and Cold Storage Using Phase Change Materials in Domestic Refrigeration Systems: The State-of-the-Art Review," *Energy and Buildings* 106 (2015): 111–124, <https://doi.org/10.1016/j.enbuild.2015.06.016>.
54. C. Veerakumar and A. Sreekumar, "Phase Change Material Based Cold Thermal Energy Storage: Materials, Techniques and Applications—A Review," *International Journal of Refrigeration* 67 (2016): 271–289, <https://doi.org/10.1016/J.IJREFRIG.2015.12.005>.
55. Cool Sarl, *Cool—The Insulated Box.com—Cool—theinsulatedbox.com* (2024), accessed April 2, 2024, <https://www.theinsulatedbox.com/>.
56. Cool Sarl, *Eutectic Gel Pouches—Cool—theinsulatedbox.com* (2024), accessed April 2, 2024, <https://www.theinsulatedbox.com/41-eutectic-gel-pouches>.
57. Cool Sarl, *Eutectic Pouch Gel 200GR-21°C—Frozen Gel Pack—Frozen Cooler* (2024), accessed April 2, 2024, <https://www.theinsulatedbox.com/eutectic-gel-pouches-/783-eutectic-gel-pack-x100-200g-21c-3347613520219.html>.
58. Cool Sarl, *Eutectic Pouch Gel 200G-12°C—Fresh Gel Pack—Fresh Cooler* (2024), accessed April 2, 2024, <https://www.theinsulatedbox.com/eutectic-gel-pouches-/646-eutectic-gel-pack-x100-200g-12c-3347613520127.html>.
59. "Technical Data Sheet of savE® HS21N," published, 2021, https://plussat.eu/wp-content/uploads/2024/04/Doc-599-TDS_HS-21N.pdf.
60. "Rubitherm Sp-21 Data Sheet," published, 2022, https://www.rubitherm.eu/media/products/datasheets/Techdata_-SP-21_EN_12072022.PDF.
61. "PCM Products—PlusICE—Subzero Eutectic PCMs," published, 2021, <https://www.pcmproducts.net/files/PlusICE%20Range%202021-1.pdf>.
62. "Cold Chain—Insolcorp, LLC," accessed February 6, 2025, <https://insolcorp.com/cold-chain-pcm-solutions/>.
63. "Technical Data Sheet of savE® HS10N," published, 2022, https://plussat.eu/wp-content/uploads/2023/06/Doc-011_PCM_HS10N-TDS.pdf.
64. "Rubitherm SP-11 Data Sheet," published, 2022, https://www.rubitherm.eu/media/products/datasheets/Techdata_-SP-11_EN_12072022.PDF.
65. K. Azzouz, D. Leducq, and D. Gobin, "Performance Enhancement of a Household Refrigerator by Addition of Latent Heat Storage," *International Journal of Refrigeration* 31 (2008): 892–901, <https://doi.org/10.1016/j.ijrefrig.2007.09.007>.
66. K. Azzouz, D. Leducq, and D. Gobin, "Enhancing the Performance of Household Refrigerators With Latent Heat Storage: An Experimental Investigation," *International Journal of Refrigeration* 32 (2009): 1634–1644, <https://doi.org/10.1016/j.ijrefrig.2009.03.012>.
67. B. Gin and M. M. Farid, "The Use of PCM Panels to Improve Storage Condition of Frozen Food," *Journal of Food Engineering* 100 (2010): 372–376, <https://doi.org/10.1016/j.jfoodeng.2010.04.016>.
68. B. Gin, M. M. Farid, and P. K. Bansal, "Effect of Door Opening and Defrost Cycle on a Freezer With Phase Change Panels," *Energy Conversion and Management* 51 (2010): 2698–2706, <https://doi.org/10.1016/j.enconman.2010.06.005>.
69. B. Gin, M. M. Farid, and P. Bansal, "Modeling of Phase Change Material Implemented into Cold Storage Application," *HVAC&R Research* 17 (2011): 257–267, <https://doi.org/10.1080/10789669.2011.572222>.
70. S. J. Sekhar, M. A. F. Raj, P. S. Raveendran, and P. C. Murugan, "Cladding Phase Change Materials in Freezing and Chilling Zones of Household Refrigerator to Improve Thermal Performance and Environmental Benefits," *Journal of Energy Storage* 55 (2022): 105476, <https://doi.org/10.1016/J.EST.2022.105476>.
71. O. Ghahramani Zarabad and R. Ahmadi, "Employment of Finned PCM Container in a Household Refrigerator as a Cold Thermal Energy Storage System," *Thermal Science and Engineering Progress* 7 (2018): 115–124, <https://doi.org/10.1016/j.tsep.2018.06.002>.
72. Sachet De Gel Eutectique 200GR-21°C, "Gel Cold Pack—Gel Refrigerant," accessed February 5, 2025, <https://www.coolerbox.com/accumulateurs-thermiques/783-gel-eutectique-x100-200g-21c-3347613520219.html>.
73. Eutectic Gel Bag, "Cold Accumulator 200g –12°C Ice Pack," accessed February 5, 2025, <https://www.coolerbox.com/accumulateurs-thermiques/646-gel-eutectique-x100-200g-12c-3347613520127.html>.

74. S. Tavman, S. Kumcuoglu, and V. Gaukel, "Apparent Specific Heat Capacity of Chilled and Frozen Meat Products," *International Journal of Food Properties* 10 (2007): 103–112, <https://doi.org/10.1080/10942910600755151>.
75. EN 16825:2016, "Refrigerated Storage Cabinets and Counters for Professional Use—Classification," published 2016, https://standards.iteh.ai/catalog/standards/cen/8376636d-c012-49c9-b3ab-a95b2ac20537/en-16825-2016?srsId=AfmBOorhcf_TQXXpcvDY5nW9GBs05VOccCcLyHipa_p6glNGA6SYEiz.
76. EN 16825:2016, "Refrigerated Storage Cabinets and Counters for Professi," 2016, https://www.intertekinform.com/en-gb/standards/en-16825-2016-342042_saig_cen_cen_783397/?srsId=AfmBOornRtQ1QxrUaD3NMnEYUMLRx2eR0rvKvg_6jAhwAywVjrRl8kHs.
77. General Specifications, *Data Acquisition System GM* (2024), accessed November 14, 2024, <https://web-material3.yokogawa.com/GS04L55B01-01EN.pdf>.
78. PFA7411-02 ATTO D4 RS485 230-240V Transducer/Energy Analyzer, "Electrex—The Energy Saving Technology," published 2015, <https://www.electrex.it/en/products/intelligent-transducers/pfa7411-02-atto-d4-rs485-230-240v-transducer-energy-analyzer.html>.
79. EN 62552:2013, "Household Refrigerating Appliances—Characteristics and Test Methods," published 2013, https://shop.standards.ie/en-ie/standards/en-62552-2013-352101_saig_cenelec_cenelec_803515/.
80. EN 62552:2013, "Household Refrigerating Appliances—Characteristics and Test Methods," published 2013, <https://standards.iteh.ai/catalog/standards/clc/19cf1403-1cc7-4eff-83a3-f61698764410/en-62552-2013>.
81. EN 62552:2013, "Household Refrigerating Appliances—Characteristics and Test Methods—nlfnorm.cz," 2014, <https://www.nlfnorm.cz/en/ehn/481>.
82. E. Oró, A. de Gracia, and L. F. Cabeza, "Active Phase Change Material Package for Thermal Protection of Ice Cream Containers," *International Journal of Refrigeration* 36 (2013): 102–109, <https://doi.org/10.1016/j.ijrefrig.2012.09.011>.